

We are IntechOpen, the world's leading publisher of Open Access books Built by scientists, for scientists

6,900

Open access books available

185,000

International authors and editors

200M

Downloads

Our authors are among the

154

Countries delivered to

TOP 1%

most cited scientists

12.2%

Contributors from top 500 universities



WEB OF SCIENCE™

Selection of our books indexed in the Book Citation Index
in Web of Science™ Core Collection (BKCI)

Interested in publishing with us?
Contact book.department@intechopen.com

Numbers displayed above are based on latest data collected.
For more information visit www.intechopen.com



Review of Recent Developments in CO₂ Capture Using Solid Materials: Metal Organic Frameworks (MOFs)

Mohammed Mohamedali, Devjyoti Nath, Hussameldin Ibrahim and Amr Henni

Additional information is available at the end of the chapter

<http://dx.doi.org/10.5772/62275>

Abstract

In this report, the adsorption of CO₂ on metal organic frameworks (MOFs) is comprehensively reviewed. In Section 1, the problems caused by greenhouse gas emissions are addressed, and different technologies used in CO₂ capture are briefly introduced. The aim of this chapter is to provide a comprehensive overview of CO₂ adsorption on solid materials with special focus on an emerging class of materials called metal organic frameworks owing to their unique characteristics comprising extraordinary surface areas, high porosity, and the readiness for systematic tailoring of their porous structure. Recent literature on CO₂ capture using MOFs is reviewed, and the assessment of CO₂ uptake, selectivity, and heat of adsorption of different MOFs is summarized, particularly the performance at low pressures which is relevant to post-combustion capture applications. Different strategies employed to improve the performance of MOFs are summarized along with major challenges facing the application of MOFs in CO₂ capture. The last part of this chapter is dedicated to current trends and issues, and new technologies needed to be addressed before MOFs can be used in commercial scales.

Keywords: CO₂ capture, solid sorbent, MOFs, ZIFs

1. Introduction

1.1. Environmental problem and CO₂ emissions

The increasing level of CO₂ emission is considered one of the major environmental challenges that our planet is facing today. The concentration of greenhouse gases in the atmosphere reached a new record in 2013, with CO₂ at 396 ppm which represents 142% of the concentration of the pre-industrial era [1]. Findings of a recent global atmosphere watch reported in a

greenhouse gas bulletin [1] revealed that CO₂ concentration has increased between 2012 and 2013, more than any other year since 1984, which was attributed to the reduced uptake by the earth's biosphere. This alarming level of CO₂ shows the urgency for taking immediate actions to prevent serious repercussions of climate change. On December 2015, at the Paris Climate Conference (COP21), 195 countries adopted a historical and the first legally binding global climate agreement to keep the increase in global average temperature to well below 2°C above pre-industrial levels. The discovery of new fossil fuel reserves, combined with rising energy demand, led to an increase in the number and capacities of power plants worldwide. This situation is expected to extend into the future due to various factors such as industrial development and economic growth, especially in developing nations, which in turn is expected to further contribute to increasing levels of greenhouse gas emissions in years to come. According to a recent report by the Energy Information Administration, energy consumption is projected to rise by 56% between 2010 and 2040. Fossil fuels will continue to supply about 80% of the world energy through 2040. Industrial energy consumption represents the greatest share of emissions and is projected to consume more than 50% of the energy delivered in 2040. According to currently implemented regulations regarding fossil fuels, CO₂ emissions from power plants is projected to increase by 46% compared to emission level in 2010 [2].

Among several approaches that could be used to overcome the greenhouse gas effect is the utilization of clean energy alternatives which could be the ultimate solution to the climate change problem in terms of reducing CO₂ emissions. However, these green technologies still require significant modifications to the current energy framework. The great challenges facing these green technologies lie in the difficulty for implementation at industrial scale, which makes it economically infeasible when compared to fossil fuel-based power plants. This implies that unless green energy alternatives and energy infrastructure for the commercialization and the implementation of these new technologies are attained, the pursuit of new CO₂ emission reduction technologies will continue to be the most practical method to address greenhouse gas effects until the advancement in clean energy technologies reaches commercial stages.

There are three different strategies to reduce emissions of CO₂ from fossil fuel-based power plants. These include post-combustion capture in which CO₂ is separated from the combustion flue gas stream that is mainly composed of nitrogen and some other minor components such as water vapor and oxygen. The separation process in this scheme is a downstream unit which allows for an easy retrofit of a post-combustion capture unit to an existing power plant. However, the limitations of this technique include a low CO₂ partial pressure, relatively high flue gas temperature and large quantities of CO₂ in the flue gas stream [3, 4]. In the pre-combustion capture scenario, the fossil fuel is treated under certain temperature and pressure to gasify the fuel and produce hydrogen. This method offers streams with high CO₂ partial pressure and thus easy separation by utilizing variety of solvents; however, it requires significant modifications to the power generation plant. The last scenario is called the oxy-fuel capture in which the fuel is burned under a pure oxygen environment which requires the separation of oxygen/nitrogen from an air stream. The process produces pure CO₂ and water vapor which can be easily recovered through a simple condensation unit. Each separation

scenario requires a different capture technology, and therefore the properties, characteristics, and operation of the separation process are also entirely different among the three strategies. The most advanced process for implementation in the field is post-combustion. We will therefore, in this chapter, focus on the post-combustion separation applications.

1.2. Existing technologies for CO₂ capture

In order to locate metal organic frameworks (MOFs) on the map of the technologies used for CO₂ capture applications, we will briefly describe the major technologies that have been employed and discuss their advantages and limitations. Figure 1 shows the different technologies used for CO₂ capture, whereas MOFs are used under the category of membranes and adsorbents.

The most widely investigated technology for CO₂ capture from flue gas is absorption using aqueous amine solutions such as monoethanolamine (MEA), diethanolamine (DEA), and methyldiethanolamine (MDEA), as well as blends of different amines [5–7]. Amine scrubbers are considered a well-developed technology and is available in commercial scale for post-combustion capture applications [8]. The major limitations of this technology include the high energy required for solvent regeneration, stability of the amine system at the regeneration conditions, and the negative influence of impurities present in the flue gas that might significantly affect the stability and performance of the solvent [9, 10].

Under the category of absorption technology and in order to overcome the limitations of amine-based technologies, aqueous ammonia as a solvent for CO₂ separation has also been widely used to benefit from the low heat of absorption of ammonia-based solvents as compared to amine systems. Besides, the ammonia can also absorb other impurities existing in the gas stream such as NO and SO_x. The major drawback of ammonia-based solvents lies in the need to cool the flue gas prior to introducing it to the absorption column to prevent ammonia losses to the gas stream. This adds a huge energy requirement considering the large volume of flue gas stream that typically needs to be treated [11]. The chilled ammonia process faces similar issues in addition to fouling of the heat exchanger by ammonium bicarbonate deposition from saturated solutions [4].

Great efforts have been made to find new and efficient materials for absorptive CO₂ separation. Ionic liquids (ILs) are liquid salts composed of cations and anions, have been proposed as promising solvents to replace the existing amine-based solvents. ILs possess several remarkable properties that make their application in CO₂ separation one of the hottest research topics in the last few years [12–14]. These properties include low volatility, high CO₂ solubility, good thermal stability, and the possibility of systematically tuning the structure toward certain properties [15–17]. Several review papers reporting experimental data related to CO₂ solubility, selectivity, effect of ILs structure on performance, and the stability of ILs are available [12, 18]. Recent developments on the application of the amine-modified ILs, known as task-specific ILs (TSILs), are also widely discussed in the literature [19, 20], including both physical and chemical interactions with CO₂. Unfortunately, many ILs and TSILs suffer from a common problem of high viscosity after CO₂ absorption. Even though some recent reports mentioned the availability of ILs with low viscosities, it is still evident that much work has to be done to

overcome this limitation. Finding cheap routes for the synthesis of these materials is one of the greatest challenges facing researchers working in this area [21]. In this chapter, a great portion will be dedicated to the incorporation of ILs into the pores of MOFs to improve their CO₂ capture capabilities.

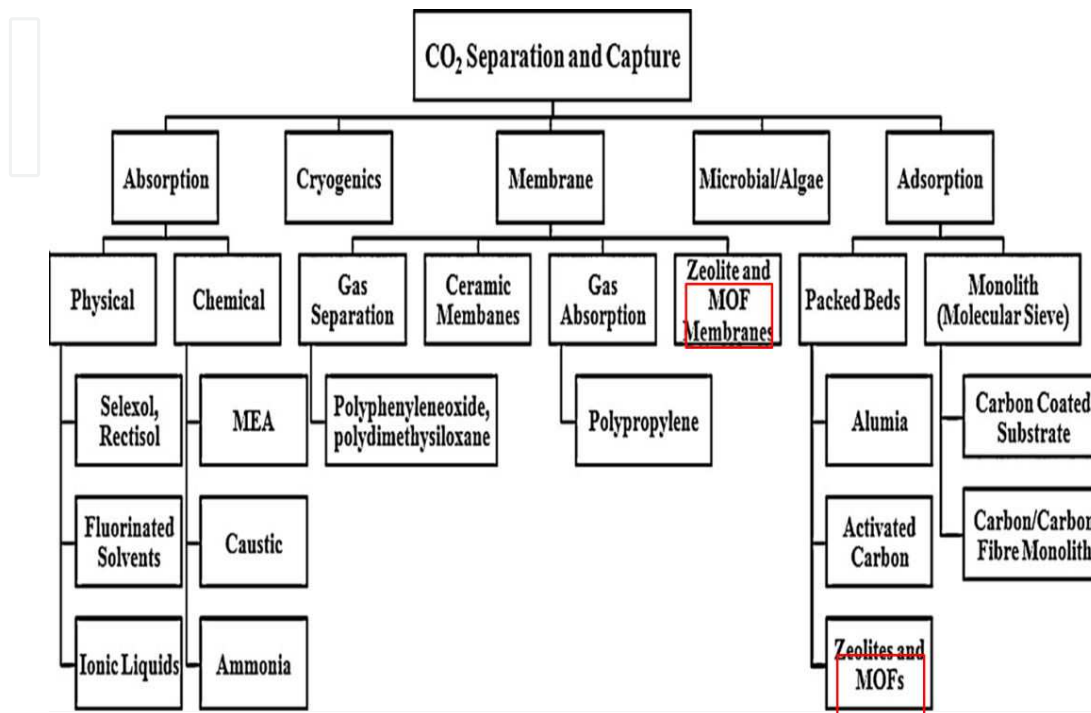


Figure 1. Different technologies used for CO₂ capture [22].

2. CO₂ capture using solid sorbents

2.1. Criteria for the evaluation of solid sorbents

In order to evaluate solid materials for their performance in CO₂ separation from flue gases, some important performance criteria must be met. These include:

- **Adsorption capacity:** it is a key criteria in evaluating solid sorbent performance. It provides information on the amount of CO₂ that could be adsorbed by a given solid material. It can be represented in terms of gravimetric uptake which is the amount of CO₂ adsorbed per unit mass sorbent (gram CO₂/gram sorbent, or cm³ CO₂/gram sorbent). The volumetric uptake is another measure for capacity, and it reports the CO₂ uptake per volume of sorbent material (gram CO₂/cm³ sorbent, or cm³ CO₂/cm³ sorbent). This criterion is of great importance because it represents the amount of sorbent needed for a particular duty and therefore the size of the adsorption bed. It is also considered a crucial factor in determining the energy requirement during the regeneration step.

- **Selectivity for CO₂:** it represents the CO₂ uptake ratio to the adsorption of any other gas (typically nitrogen for post-combustion capture, and methane for natural gas). It is an essential evaluation criterion, and affects the purity of the adsorbed gas, which will significantly influence the sequestration of CO₂. The simplest method to estimate the selectivity factor is to use single-component adsorption isotherms of CO₂ and nitrogen.
- **Enthalpy of adsorption:** it represents another critical parameter in the evaluation of the performance of solid sorbents. It is a measure of the energy required to regenerate the solid sorbent, and it therefore significantly influences the cost of the regeneration process. It represents the affinity of the material toward CO₂ and measures the strength of the adsorbate–adsorbent interaction.
- **Physical, thermal, and chemical stability:** in order to reduce operating costs, solid sorbents must demonstrate stability under flue gas conditions, adsorption operation conditions, and during the multi-cycle adsorption–regeneration process. In particular, stability in the presence of water vapor is essential for the sustainable performance of the solid sorbent. In addition to thermal properties of the solid sorbent, heat capacity and thermal conductivity are also important in heat transfer operations.
- **Adsorption/desorption kinetics:** the time of the adsorption–regeneration cycle greatly depends on the kinetics of the CO₂ adsorption–desorption profile, which is measured in breakthrough experiments. Sorbents that adsorb and desorb CO₂ in a shorter time are preferred as these reduce the cycle time as well as the amount of sorbent required, and ultimately the cost of CO₂ separation.
- **Cost of the sorbent material:** it is an important factor in the selection of the sorbent material. Materials that exhibit excellent adsorption attributes, and are readily available at low cost, are considered the main targets for researchers working in the field of CO₂ capture. Besides, the environmental impact of synthesizing these materials is considered one of the greatest challenges to overcome.

In the following sections, we describe the main solid sorbents used for CO₂ capture, their applications, major attributes, and limitations.

2.2. Zeolites

Zeolites are porous crystalline aluminosilicate materials available naturally, but can also be prepared synthetically. The zeolite framework is composed of tetrahedral T atoms where T could be Si or Al, connected by oxygen atoms to form rings of different pore structures and sizes. The pore size of the zeolite framework varies between 5 and 12 Å [23]. They are widely used as catalysts in the refining industry [24, 25], fine chemicals synthesis [26, 27], and in gas separation applications [28, 29]. Zeolites are considered promising candidates in CO₂ capture application as has been widely reported in the literature [30–32]. CO₂ can be adsorbed on zeolites through different mechanisms, such as molecular sieving effect based on the difference in size [33, 34]. Separation can also take place based on polarization interactions between the gas molecule and the electric field on the charged cations in the zeolite framework [33]. Accordingly, CO₂ removal with zeolites can be controlled by changing the pore size, polarity,

and the nature of the extra framework cation. Among the different zeolites investigated for CO₂ capture applications, zeolite 13X is the most widely studied sorbent, and is considered the benchmark technology for solid sorbents [35, 36]. Research on the use of zeolites as sorbents for CO₂ capture can be categorized into different areas depending on the approach and the techniques adopted to address the improvement in capture performance. These categories comprise tuning the pore size, designing zeolites with controlled polarities, investigating novel zeolites, optimizing the cation exchange, and most recently incorporating amine moieties and other chemical functions into the zeolite frameworks. Ocean et al. [37] have studied the selectivity to adsorb CO₂ by controlling the pore size of an NaKA zeolite through the synthesis of nanosized NaKA zeolites. Overall, the adsorption kinetics on the nanosized crystals was fast enough for CO₂ capture applications; however, the formation of a thin layer on the nanosized NaKA zeolite, due to intergrowth on the surface, did not considerably improve the adsorption kinetics. In contrast, Goj et al. [38] performed atomistic simulations for silicalite, ITQ-3, and ITQ-7, and reported a positive effect on CO₂ uptake and selectivity by tuning the pore apertures. Sravanthi et al. [39] provided a novel approach to control the pore size and volume by utilizing pore expansion agents and obtained average pore size around 30 nm. The application of the pore-expanded MCM-41 in CO₂ separation resulted in the uptake of about 1.2 mmol/g.

Several studies have been conducted to control zeolite affinity toward CO₂, which can be realized by tuning the polarity of the zeolite through alteration of the Si/Al ratio and the nature of the cation. Remy et al. [33] studied the selective separation of CO₂ on low-silica KFI zeolite (Si/Al = 1.67) by employing ion exchange with Na, Li, and K. Li-exchanged KFI has shown the highest CO₂ uptake which was attributed to the large pore volume as compared to Na and K cations. In comparison with high-silica KFI sample (Si/Al = 3.57–3.67), Li-KFI had the highest capacity at low pressure due to the strong electrostatic field. The overlap between pore size and polarity effects is also strongly observed for amine-supported zeolites, which have gained considerable attention in the last few years [40–45]. For instance, Ahmad et al. [46] have impregnated melamine into β -zeolite and obtained dynamic CO₂ uptake of 3.7 mmol/g at atmospheric pressure and temperature of 25 °C. The major challenge facing amine-modified zeolites is the tradeoff between the increased affinity toward CO₂ (strong interaction with the sorbent) and the reduction in pore volume, and consequently the uptake, especially, at low pressures. Factors such as amines loading, distribution, and the nature of the cation can play a vital role to avoid the blockage of the porous structures with the bulky amine moieties [42, 47]. Kim et al. [48] have performed a rigorous investigation through the simulation of thousands of zeolites to evaluate the adsorption properties of these materials and identify the optimum structures for improved CO₂ separation attributes. This study provides a systematic approach to rank and select appropriate zeolites for the required capture objectives. However, important factors such as stability under humid environment, adsorbent and process cost, and the availability of zeolite structures were not taken into consideration.

The hydrophilic nature of most zeolite structures is considered a major drawback of zeolites especially for post-combustion CO₂ applications [49, 50]. Water competes with CO₂ on the

available sorption sites and might influence the zeolite structure and framework [51]. As explained earlier, the presence of the exposed cation sites increases CO₂ uptake. In a recent study by Serena et al. [52], the relationship between the water content of the zeolite and the density of the cations was investigated, and a linear relationship was found to describe the decrease of the cation population with increasing water content. This observation highlights the detrimental effect of the presence of water vapor on the adsorption of CO₂ on zeolites.

2.3. Carbon-based CO₂ capture

Carbon-based adsorbents have been used for CO₂ separation in different forms including activated carbons (ACs), carbon nanotubes (CNTs), and graphenes. Activated carbons have an amorphous porous structure with high surface areas that are readily available for CO₂ uptake. They have been widely investigated as sorbents for CO₂ removal due to their low cost and the availability of raw materials [53–55]. However, there are no active sites to bond with the adsorbed CO₂ as cations in zeolite sorbents. This weak interaction results in lower enthalpy and therefore lower energy requirement for regeneration. On the contrary, ACs have very low CO₂ uptake at low pressures due to the absence of the electric field on the surface. Kacem et al. [56] performed a comparison between the performance of ACs and zeolite for CO₂/N₂ and CO₂/CH₄ separation based on their capacity, regeneration capacity, and reusability. It was concluded that at higher pressures (above 4 bars), the CO₂ uptake for ACs was much higher than zeolites. Also, the recovered CO₂ after the regeneration of ACs had higher purity than in the case of zeolites. When compared to zeolites, ACs maintain their adsorption stability even in the presence of water vapor which does not cause any framework failure [57].

In order to enhance the adsorption capacity on ACs, several studies have been conducted in order to improve the affinity toward CO₂ by introducing amine-based functional groups [58–61]. In a recent study, Maria et al. [62] described a systematic surface modification of microporous ACs through a stepwise chemical treatment. They were successful in grafting amine and amide functional groups on the surface of ACs with only 20% loss of surface area. Gibson et al. [63] studied the polyamine-impregnated porous carbons and achieved 12 times higher CO₂ capacity than bare porous carbon. Chitosan and triethylenetetramine have been successfully impregnated onto the surface of ACs and have shown 60 and 90% increased CO₂ uptake at 298 K and 40 bars. In addition to amine functional groups, ammonia-modified ACs, at atmospheric pressure and a temperature range from (303 to 333) K, have been studied [64]. Authors report that an enthalpy of 70.5 kJ/mol was obtained compared to 25.5 kJ/mol for the pristine ACs, suggesting the possibility of chemisorption. Another report has also supported the improved adsorption capacity and selectivity by employing NH₃ at high temperature and has considerably improved CO₂ uptake from 2.9 mmol/g for the bare AC to 3.22 mmol/g for the modified one at 303 K and 1 bar.

Several studies have been dedicated to the application of amine-modified carbon nano tubes (CNTs) as solid sorbents for CO₂ separation [65–69]. Industrial grade CNTs have been functionalized with tetraethylenepentamine (TEPA) by Liu et al. [65], and the effects of amine loadings on the CO₂ uptake, heat of adsorption, and adsorbent regenerability were investi-

gated. TEPA-impregnated CNTs have shown an enhanced capacity of 3.09 mmol/g at 343 K. Similar studies were also reported using different amines such as (3-aminopropyl)triethoxysilane (APTES) [70], polyethyleneimine (PEI) [67], and other amines (primary, secondary, tertiary, diamines, and tri-amines) [71].

Graphene is a planar sheet of carbon atoms extended in two dimensions, and was discovered in 2004 [72]. Graphite-based capture was recently introduced (after 2011) as a promising candidate for CO₂ capture applications, and research is growing rapidly in this area [73–77]. A recent review by Najafabadi is available on the current status and research trends of using graphene and its derivatives as solid sorbents for CO₂ capture [78]. Research in this area involves grafting various functional groups on graphene such as N-doped graphene composites (surface area = 1336 m²/g), as reported by Kemp et al. [79], which showed a reversible CO₂ capacity of 2.7 mmol/g at 298 K and 1 atm as well as enhanced stability for repeated adsorption cycles. Borane-modified graphene was also reported by Oh et al. [80], obtaining a CO₂ uptake of 1.82 mmol/g at 298 K and 1 atm. Some novel hybrid materials have also been introduced to obtain better improvements in the adsorption properties, including mesoporous graphene oxide (GO)-ZnO nanocomposite [81], mesoporous TiO₂/graphene oxide nanocomposites [82], Mg–Al layered double hydroxide (LDH), graphene oxide [83], MOF-5 and aminated graphite oxide (AGO) [84], UiO-66/graphene oxide composites [85], and MIL-53(Al) and its hybrid composite with graphene nanoplates (GNP) [86].

2.4. Metal organic frameworks

A more recent class of porous materials was manufactured and named metal organic frameworks. They represent one of the promising adsorbents and have gained significant attention during recent years for gas separation applications [87, 88]. MOFs are composed of metal ions or clusters (nodes) bridged by organic ligands (connectors) to form various structures and networks. MOFs are well recognized for their extraordinary surface areas, ultrahigh porosity, and most importantly the flexibility to tune the porous structure as well as the surface functionality due to the presence of organic ligands that can easily be chemically modified [89, 90]. One main advantage of MOFs over other solid materials is the possibility to tailor the pore size and functionality by rational selection of the organic ligand, functional group, metal ion, and activation method.

Several review papers are available in the literature for gas separation using MOFs [91–96]; however, great progress has been achieved during the past four years (2012 onward). In order to address the limitations of MOFs and investigate new structures, novel functional groups, in addition to hybrid systems and technologies, more studies are needed to explore the mechanisms involved and to improve the uptake capacity in a humid environment. For these reasons, considerable effort has been observed during the past decade to address gas separation and adsorption using MOFs. Figure 2 shows the number of publications on CO₂ capture and separation using MOFs during the past 15 years, which reflects the growing interest of MOFs as efficient solid sorbents.

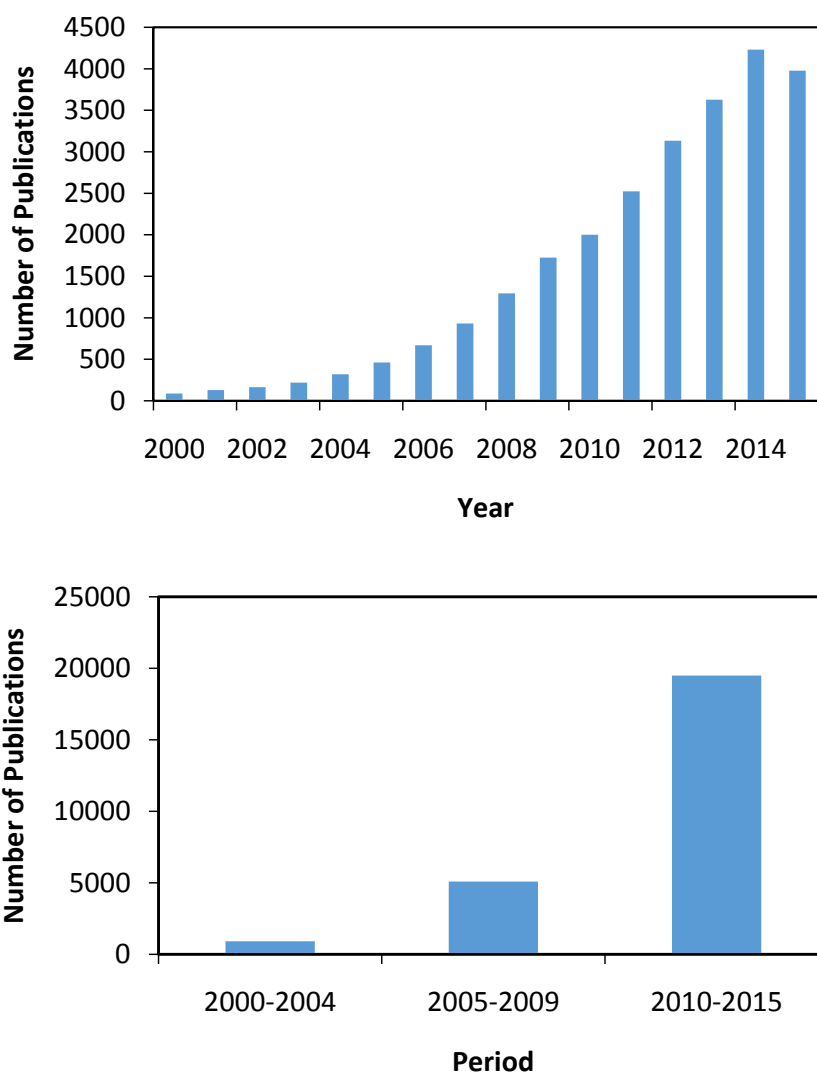


Figure 2. Number of publications on CO₂ capture using MOFs (based on Web of Science database)

3. Adsorption of CO₂ on metal organic frameworks

CO₂ capture performance of different MOFs will be comprehensively reviewed in terms of their capacity, selectivity, heat of reaction, and major challenges facing researchers, and some ideas to approach these challenges will also be provided. The next section is dedicated to review the most recent studies of CO₂ capture and separation on MOFs, and we will mainly target the works published in the last four years.

3.1. Evaluation of MOFs in CO₂ Capture

As introduced earlier, capacity, selectivity, and heat of adsorption are considered the main criteria for the evaluation of MOFs for CO₂ separation. CO₂ uptake is a proportional function

of pressure in the gas phase, where the low pressure corresponds to post-combustion applications. The gravimetric uptake of CO₂ is indicative of the ability of MOFs to adsorb CO₂ and, therefore, we have reported CO₂ uptake along with MOF surface area, and other properties for MOFs published after 2012 which could be added to the published reviews that have listed these data in a table format. Table 1 represents the properties of MOFs at high-pressure applications, while Table 2 presents the low-pressure data.

Common name	Surface Area (m ² /g)		Capacity (wt%)	Pressure (bar)	Temp. (K)	Selectivity	Q _{st} (kJ/mol)	Ref.
	BET	Langmuir						
UiO(bpdc)	2646	2965	72.5	20	303			[97]
ZJU-32	3831		49	40	300			[98]
UPG-1	410	514	11.9	9.8	298	24	24	[99]
Cu ₃ (H ₂ L ²)(bipy) ₂ ·11H ₂ O			6.4	8.5	298			[100]
Cu ₃ (H ₂ L ²)(etbipy) ₂ ·24H ₂ O			4.7	9.6	298			[100]
NU-111	4932		61.8	30	298		23	[101]
HTS-MIL-101	3482		52.8	40	298			[102]
DGC-MIL-101	4198		59.8	40	298			[102]
UTSA-62a	2190		43.7	55	298		16	[103]
ZIF-7	312	355	20.9	10	298		33	[104]
{Ag ₃ [Ag ₅ (l3-3,5-Ph ₂ tz) ₆] (NO ₃) ₂] _n			12.3	10	298	10.5	19.1	[105]
{Ag ₃ [Ag ₅ (l3-3,5-tBu ₂ tz) ₆] (BF ₄) ₂] _n			5.4	10	298	14	15	[105]
Basolite® C 300	1706.42		41.9	224.99	318		18	[106]
Basolite® F300	1716.46		24.1	224.99	318		19	[106]
Basolite® A100	1524.8		26.9	224.99	318		9	[106]
IRMOF-8	1599	1801	7.8	1	298		21.1	[107]
IRMOF-8-NO ₂	832	926	3.8	1	298		35.4	[107]
MIL-101(Cr)	2549		24.2	30	303			[108]
HKUST-1	1326		26.3	30	303			[108]
DMOF	1980		38.1	20	298	12 ^a	20	[109]
DMOF-DM1/2	1500		27.5	20	298			[109]
DMOF-Br	1320		24.3	20	298			[109]
DMOF-NO ₂	1310		32	20	298			[109]

Common name	Surface Area (m ² /g)		Capacity (wt%)	Pressure (bar)	Temp. (K)	Selectivity	Qst (kJ/mol)	Ref.
	BET	Langmuir						
DMOF-TM1/2	1210		23.9	20	298			[109]
DMOF-TF	1210		16.2	20	298	9 ^a	18	[109]
DMOF-CI2	1180		26.4	20	298	17	21	[109]
DMOF-OH	1130		24.8	20	298			[109]
DMOF-DM	1120		25.4	20	298	23 ^a	23	[109]
DMOF-TM	1050		23.6	20	298	28 ^a	29	[109]
DMOF-A	760		17.1	20	298			[109]

^a IAST selectivity

Table 1. Adsorption capacities at high pressure

Common name	Surface Area (m ² /g)		Capacity (wt%)	Pressure (bar)	Temp. (K)	Selectivity	Qst (kJ/mol)	Ref.
	BET	Langmuir						
rht-MOF-pyr	2100		12.7	1	298		28	[110]
rht-MOF-1	2100		11	1	298		29	[110]
JLU-Liu22	1487		15.6	1	298		30	[111]
SIFSIX-3-Zn			8.9	1	298			[112]
SIFSIX-3-Cu			9.6	1	298			[112]
SIFSIX-3-Co	223		10	1	298		47	[112]
SIFSIX-3-Ni	368		10.3	1	298		51	[112]
{[H ₂ N(CH ₃) ₂] ₄ [Zn ₉ O ₂ (BTC) ₆ (H ₂ O) ₃ .3DMA]c _n }	844	1132	10.9	0.91	298		29	[113]
{[NH ₂ (CH ₃) ₂ Cd(BTC)].DMA] _n }	406	539	6.4	0.91	298	30	34.7	[113]
Ni-DOBDC	798		18.2	1	298			[114]
Py-Ni-DOBDC	409		12	1	298			[114]
UiO(bpdc)	2646	2965	8	1	303			[97]
ZJU-32	3831		4.8	1	300			[98]
Cu-TDPAH	1762		18.4	1	298	200 ^a	33.8	[115]
Zn/Ni-ZIF-8-1000		750	9.9	1	298	30 ^a	61.2	[116]
ZIF-8-1000			9.6	1	298	23.5 ^a	49.7	[116]

Common name	Surface Area (m ² /g)		Capacity (wt%)	Pressure (bar)	Temp. (K)	Selectivity	Qst (kJ/mol)	Ref.
	BET	Langmuir						
Zn(5-mtz)(2-eim).(guest) [ZTIF-1]	1430	1981	8.2	1	295	81	22.5	[117]
Zn(5-mtz)(2-pim).(guest) [ZTIF-2]	1287	1461	3.8	1	295		20	[117]
UTSA-49	710.5	1046.6	13.6	1	298	95.8		[118]
ZJNU-40	2209		16.4	1.01	296		18.4	[119]
UPG-1	410	514	2.1	1	298	24	24	[99]
InOF-8			6.9	1	295	45.2		[120]
Cu ₃ (H ₂ L ¹)(bipy) ₂ ·9H ₂ O			2.5	1	195			[100]
Cu ₃ (H ₂ L ²)(bipy) ₂ ·11H ₂ O			2.3	1	298			[100]
Cu ₃ (H ₂ L ²)(etbipy) ₂ ·24H ₂ O			0.5	1	298			[100]
UiO-66(Zr100)	1390	1644	6.2	1	298		26	[121]
UiO-66(Ti32)	1418	1703	6.4	1	298		28	[121]
UiO-66(Ti44)	1749	2088	7.2	1	298		34	[121]
UiO-66(Ti56)	1844	2200	8.8	1	298		37	[121]
NU-111	4932		4.8	1	298		23	[101]
JLU-Liu1	145	221	5.9	1	298		47.7	[122]
HTS-MIL-101	3482		12.3	1	298			[102]
DGC-MIL-101	4164		14.5	1	298			[102]
UNLPF-1			13.9	1	273			[123]
UTSA-62a	2190		8.1	1	298		16	[103]
[Zn ₂ (BME-bdc) _x (DB-bdc) _{2-x}] _n			21.7	0.91	195			[124]
Zn-DABCO	1870	1902	7.2	1	298		22.4	[125]
Ni-DABCO	2120	2219	8.1	1	298		25.8	[125]
Cu-DABCO	1616	1678	6.2	1	298		22.4	[125]
Co-DABCO	2022	2095	4.1	1	298		29.8	[125]
ZnAcBPDC	920		11.7	0.9	293			[126]
ZnBuBPDC	850		7.6	0.89	293			[126]
Mg/DOBDC	1415.1		25	1	298		47	[127]
Co/DOBDC	1089.3		21.6	1	298		37	[127]

Common name	Surface Area (m ² /g)		Capacity (wt%)	Pressure (bar)	Temp. (K)	Selectivity	Qst (kJ/mol)	Ref.
	BET	Langmuir						
Ni/DOBDC	1017.5		20.5	1	298		42	[127]
MIL-100(Cr)	1528.7		9.5	1	298			[127]
ZIF-7	312	355	9.1	1	298			[104]
{Ag ₃ [Ag ₅ (1,3-3,5-Ph ₂ tz) ₆](NO ₃) ₂] _n			1.6	1	298	10.5	19.1	[105]
{Ag ₃ [Ag ₅ (1,3-3,5-tBu ₂ tz) ₆](BF ₄) ₂] _n			1.6	1	298	14	15	[105]
CuBTTri	1700		10.8	1	293			[128]
pip-CuBTTri	380		7.1	1	293	130 ^a	96.5	[128]
Basolite® C 300	1706.42		9.4	0.95	318		18	[106]
Basolite® F300	1716.46		2.4	0.95	318		19	[106]
Basolite® A100	1524.8		4.4	0.95	318		9	[106]
IRMOF-8	1599	1801	51.2	30	298		21.1	[107]
IRMOF-8-NO ₂	832	926	31.3	30	298		35.4	[107]
CPM-5	2187		8.8	1	298	16.1	36.1	[129]
Ni-MOF-74	1252	1841	19.4	1	298			[130]
Mg-MOF-74	1416	2085	30.1	1	298			[130]
MIL-101(Cr)	2549		6.8	1	303			[108]
HKUST-1	1326		13.2	1	303			[108]
[Cu(tba) ₂] _n			7.3	1	293	25 ^a	36.0	[131]
IRMOF-74-III-CH ₃	2640		10	1	298			[132]
IRMOF-74-III-NH ₂	2720		10.4	1	298			[132]
IRMOF-74-III-CH ₂ NHBoc	2170		7	1	298			[132]
IRMOF-74-III-CH ₂ NMeBoc	2220		6.6	1	298			[132]
IRMOF-74-III-CH ₂ NH ₂	2310		10.8	1	298			[132]
IRMOF-74-III-CH ₂ NHMe	2250		9.6	1	298			[132]
DMOF	1980			1	298	12 ^a	20	[109]
DMOF-DM1/2	1500		8.1	1	298			[109]
DMOF-Br	1320		6.4	1	298			[109]

Common name	Surface Area (m ² /g)		Capacity (wt%)	Pressure (bar)	Temp. (K)	Selectivity	Qst (kJ/mol)	Ref.
	BET	Langmuir						
DMOF-NO ₂	1310		9.9	1	298			[109]
DMOF-TM1/2	1210		8.1	1	298			[109]
DMOF-TF	1210		3.3	1	298	9 ^a	18	[109]
DMOF-Cl ₂	1180		8.8	1	298	17 ^a	21	[109]
DMOF-OH	1130		9.6	1	298			[109]
DMOF-DM	1120			1	298	23 ^a	23	[109]
DMOF-TM	1050		13.3	1	298	28 ^a	29	[109]
DMOF-A	760		10.6	1	298			[109]
CPM-33a	966	1257	12.6	1	298		22.5	[133]
CPM-33b	808	1119	19.9	1	298		25	[133]
Ni ₃ OH(NH ₂ bdc) ₃ tpt	805	1115	14.8	1	298		21.5	[133]
Ni ₃ OH(1,4-ndc) ₃ tpt	222	310	4.6	1	298		25.3	[133]
Ni ₃ OH(2,6-ndc) ₃ tpt	1002	1392	7.9	1	298		24.7	[133]
Ni ₃ OH(bpdc) ₃ tpt	724	1009	5.5	1	298		18.7	[133]
ZIF-7-S	150		3.7	1	303			[134]
ZIF-7-D	25		9	1	303			[134]
ZIF-7-R	5		8.7	1	303		34	[134]
HKUST-1		2203	12.8	1	313			[135]
Fe-MIL-100		2990	6.6	1	313			[135]
Zn(pyrz) ₂ (SiF ₆)			10.8	1	313			[135]
Mg ₂ (dobpdc)		1940	23.8	1	313			[135]
Ni ₂ (dobpdc)		1593	21.2	1	313			[135]
m ¹ men-Mg ₂ (dobpdc)			15.8	1	313			[135]
m ¹ men-Ni ₂ (dobpdc)			7.3	1	313			[135]
m ¹ men-CuBT ₃ Tri			11.3	1	313			[135]

^a IAST selectivity

Table 2. Adsorption capacities at low pressure

3.2. Strategies to Improve the CO₂ Capture Performance on MOFs

Several strategies have been adopted to improve the performance of MOFs in CO₂ capture applications. The ability to precisely tune the MOF structures has led to versatile approaches

that can be utilized to enhance CO₂ uptake, selectivity, and the affinity toward CO₂. These methods could be classified into effects of open metal sites, pre-synthetic modifications of the organic ligand, and post-synthetic functionalization schemes.

3.2.1. Open Metal Sites

Open metal sites in MOFs are formed by the removal of a solvent molecule coordinated to the metal nodes by applying vacuum and/or heat after the synthesis of framework in a process called "activation." The presence of open metal sites on the MOF framework has a great impact on the selectivity toward CO₂ as well as on the binding energy between the adsorbed CO₂ molecules and the surface of MOF sorbents. These coordinately open metal centers act as binding sites where CO₂ molecules can attach and bind to the pore surface by the induction of dipole–quadrupole interactions. Allison et al. [136] have developed a systematic procedure to precisely understand the interactions between the CO₂ molecule and the force field generated by the open metal sites in MOF-74. The developed method allows for accurate estimation of adsorption isotherms using computational approach which enables the evaluation of different hypothetical open metal sites. These observations confirm previous findings of Kong et al. on understanding CO₂ dynamics in MOFs with open metal centers [137]. Among the MOF family, HKUST-1, M-MIL-100, M-MIL-101, and M-MOF-74 are the most widely studied frameworks with open metal sites (M represents the metal site). However, to precisely investigate the influence of the open metal sites, we need to isolate the effects of the nature of organic ligands, the synthesis route, and functional groups present in the framework. It was observed that utilizing light metal sites provides higher surface areas, and therefore improve CO₂ uptake at low pressures for MOF-74 [138]. Several studies have reported the effects of metal centers using computational approach as reported for M-MOF-74 [138–140] where noble metals such as Rh, Pd, Os, Ir, and Pt are considered promising candidates for CO₂ capture (see Figure 3).

Casey et al. [141] studied the isostructural series of HKUST-1 for various metal centers (Mo, Ni, Zn, Fe, Cu, and Cr) to get insights into the adsorption mechanism and the force field created by different metal types. It was found that the presence of divalent metals such as Mg²⁺ significantly increased CO₂ binding strength and resulted in higher selectivity toward CO₂. In addition to the nature of the metal nodes, it was found that the activation method plays a vital role in determining CO₂ uptake and affinity toward CO₂ which was in agreement with Llewellyn et al. [142] for MIL-100 and MIL-101, where various activation methods resulted in different CO₂ loadings and heat of adsorption.

In a recent study, Cabelo and coworkers [143] investigated the interaction between CO₂ and the unsaturated Cr(III), V(III), and Sc(III) metal sites in MIL-100 framework using variable temperature infrared spectroscopy. The enthalpy of adsorption for Cr(III), V(III), and Sc(III) were amounted to be (–63, –54, and –48) kJ/mol, respectively, which are considered among the highest values for CO₂ adsorption on MOFs with open metal centers to date. The synthesis and characterization of an M-DABCO series (M = Ni, Co, Cu, Zn) were described by Sumboon et al. [125] to systematically evaluate the effect of the metal identity on surface area, pore volume, and CO₂ uptake. It was concluded that Ni-DABCO has shown the highest pore volume and specific surface area due to the high charge density present at the metal center. Comparison

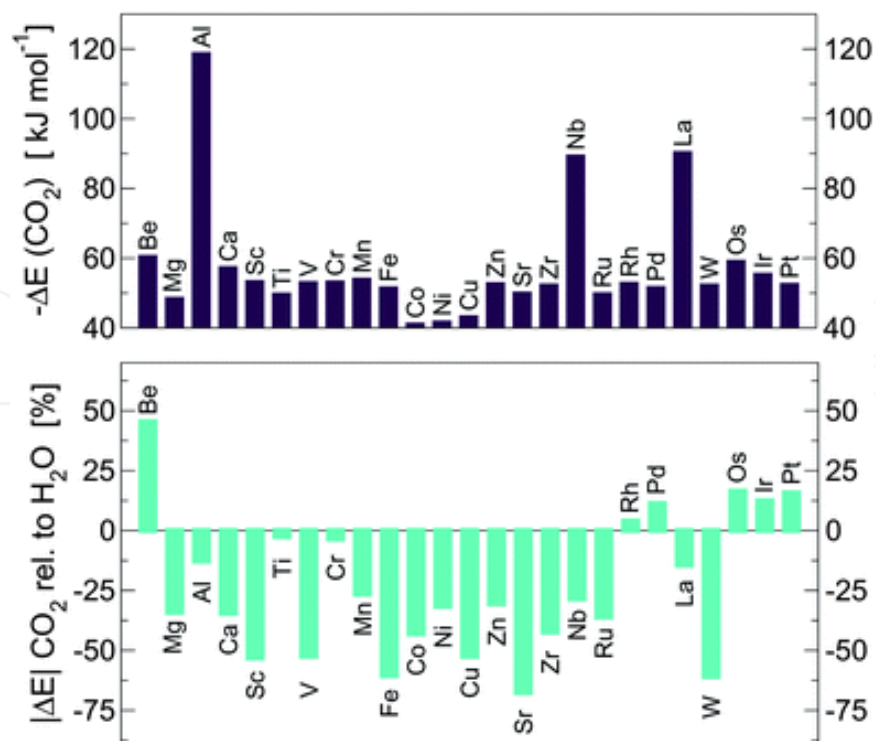


Figure 3. Top: ΔE for CO_2 adsorption (in kJ/mol) in M-MOF-74. Bottom: Magnitude of the adsorption energy of CO_2 relative to H_2O . A positive value in this plot means that CO_2 binds more strongly than H_2O (Adapted from [139]).

of the M-DABCO with activated carbons and MIL-100(Cr) revealed that the unsaturated cations possess exceptional CO_2 uptake of $180 \text{ cm}^3/\text{g}$ at 1 bar and 298 K [as compared to $30 \text{ cm}^3/\text{g}$ for ACs and $60 \text{ cm}^3/\text{g}$ for MIL-100(Cr),144].

3.2.2. Pre-synthetic Modifications of MOFs

Organic ligands are the linkers that connect the metal nodes together and therefore determine the framework structure, pore volume, pore window, and surface area which are very crucial characteristics in CO_2 separation process. Ligand functionalization is considered to be a powerful tool to improve the adsorption of CO_2 on MOFs due to the wide range of functional groups and the ease of modifying the organic ligand through strong covalent interactions. In a recent computational work by Torrissi et al., the impacts of various functional groups attached to the ligand part were investigated by density functional theory (DFT) [145]. The incorporation of amine functional moieties to the organic ligands has witnessed much attention in recent years, due to the proven positive effect of the presence of open nitrogen sites on the MOF frameworks [146]. Keceli et al. [147] studied four biphenyl ligands modified with amide groups of different chain lengths. Varying the length of the alkylamide group has shown a great impact on the porosity, surface area, and CO_2 capacity. It was also evident that the activation procedure has great influence on the surface area of the resulting material which is attributed to the different mechanisms of solvent removal from the MOF framework. Three amino-functionalized MOFs have been prepared from 2-aminoterephthalate (ABDC) and three different metals (Mg, Co, and Sr). Despite a low surface area (63, 71, and 2.5 for Mg, Co,

and Sr, respectively) and a relatively low CO₂ uptake (1.4 mmol/g at 1 bar and 298 K), the prepared MOFs had exceptional selectivity toward CO₂ (396 was recorded for Mg-ABDC) and exhibited high heat of adsorption [148]. Shimizu and coworkers [149] used 3-amino-1,2,4-triazole ligands to design a 3D structure MOF with 782 m²/g surface area and 0.19 cm³/g pore volume that is capable to achieve CO₂ uptake of 4.35 mmol/g at 1.2 bar and 273 K. Moreover, the as-synthesized MOF has shown enthalpy of adsorption of 40.8 kJ/mol at zero coverage which was comparable to the commercial zeolite NaX (48.2 kJ/mol). In a similar study, Xiong et al. [118] used triazole ligands to prepare a new framework called UTSA-49 by incorporating nitrogen atoms and methyl functional groups on 5-methyl-1H-tetrazole ligands which recorded 13.6 wt% CO₂ uptake at 1 bar and 298 K and 27 kJ/mol enthalpy (Figure 4). These observations were in agreement with work reported by Gao et al. for the influence of triazolate linkers [150]. It is essential to understand the synergistic effect between the multiple functional groups on the pore surface and their size exclusion effects which are considered potential approaches to optimize the performance of functionalized MOFs. Table 3 summarizes CO₂ capture properties of MOFs modified with different amino functional groups.

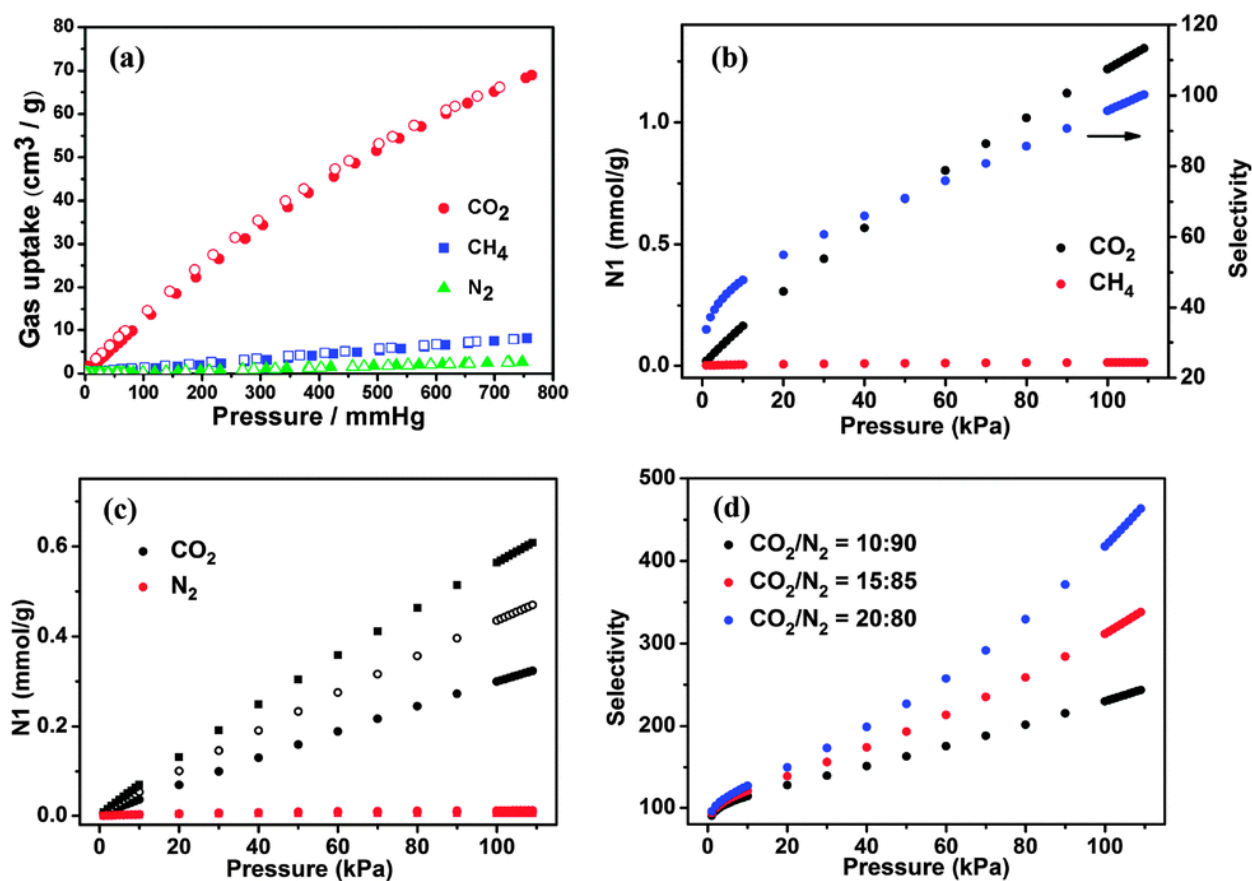


Figure 4. (a) Adsorption (solid) and desorption (open) isotherms of carbon dioxide (red circles), methane (blue squares), and nitrogen (green triangles) on UTSA-49a at 298 K. (b) Mixture adsorption isotherms and adsorption selectivity predicted by IAST of UTSA-49a for CO₂ (50%) and CH₄ (50%) at 298 K. (c) Mixture adsorption isotherms predicted by IAST of UTSA-49a for CO₂ and N₂ (10:90, 15:85, and 20:80) at 298 K. (d) Mixture selectivity predicted by IAST of UTSA-49a for CO₂ and N₂ (10:90, 15:85, and 20:80) at 298 K. Adapted from [118].

MOF name	Type of functional group	CO ₂ uptake (wt. %)	Enthalpy of adsorption (kJ/mol)	Pressure	Temperature	Surface area (m ² /g)	Ref.
ZIF-10	IM	20.9	14.9	0.9	298	-	[151]
ZIF-68	(bIM)(nIM)	41.3	33.3	0.9	298	1220	[151]
ZIF-69	(cbIM)(nIM)	38.1	25.9	0.9	298	1070	[151]
ZIF-71	dcIM	18.0	19.4	0.9	298	-	[151]
Cu ₂ (L)(H ₂ O) ₂	Pyrazol	32	-	1	195	844.5	[152]
[Zn ₂ (L)]	Pyrazol	37.4	-	1	195	1075.4	[152]
[Cd ₂ (L)]	Pyrazol	24.6	-	1	195	571.7	[152]
[Co ₂ (L)(H ₂ O) ₆]	Pyrazol	31.6	-	1	195	734.6	[152]
Zn ₄ (bpta) ₂ -1	Bipyridine pillar ligands	8.2	34.82	1.2	298	413	[153]
Zn ₄ (bpta) ₂ -1	Bipyridine pillar ligands	3.1	27.69	1.2	298	51	[153]
Cu ₂ L (DMA) ₄	Acrylamide	22.2	35	1	296	1433	[154]
Zn(ad)(ain)	2-Aminoisonicotinate and adeninate	9.2	40	1	298	399	[155]
bio-MOF-11	Adenine	22.2	33.1	1	273	1148	[156]
bio-MOF-12	Adenine	16.2	38.4	1	273	-	[156]
bio-MOF-13	Adenine	10.4	40.5	1	273	-	[156]
bio-MOF-14	Adenine	8	-	1	273	17	[156]
Cu(tba) ₂	Triazol	7.3	36	1	293	-	[131]

Table 3. CO₂ uptake for MOFs modified with amine containing ligands

Apart from amine groups, there are other functional moieties that are proven to be effective in enhancing the performance of MOFs in CO₂ capture. Phosphonate and sulfonate organic ligands have gained tremendous attention recently due to their significant improvements in MOF stability toward water [157]. Several studies are reported based on the use of phosphonate and sulfonate ligands, for instance, the selective CO₂/N₂ separation over nitrogen-containing phosphonate MOFs was studied by Marco et al. [100], and the synthesis, stability, porosity of the phosphonate MOFs [158], and their major applications were reported for water stability studies [159–161]. The shielding effect exhibited by phosphonate groups were responsible for the improved stability under humid conditions up to 90% relative humidity at 353 K as observed for CALF-30 [161]. The enhanced water stability of these MOFs was attributed to the kinetic blocking effect which makes the framework completely hydrophobic [159].

MOFs containing nitrogen-donor building blocks were also widely investigated, particularly adenine group which was extensively used due to framework robustness, richness in nitrogen sites, and framework diversity [162]. Song et al. [163] reported the preparation of three new

adenine-based MOFs by controlling the adenine coordination with Cd metal sites. This study has provided insight into the controlled synthesis of MOFs by controlling the structure building units (SBU) which can be utilized to extend the idea to include multiple building units within the same framework. Similar studies are also available based on adenine groups as building units, where the effect of the adenine functionalization on framework topology, porosity, and adsorption behavior was investigated [164]. The use of Zn-adeninate SBU led to the discovery of highly porous Bio-MOF-11 to 14 series [165] and Bio-MOF-100 [166] with exceptional surface area (4300 m²/g) and very large pore volume (4.3 cm³/g); however, the framework stability of these materials still needs to be addressed as the material tends to lose its porosity under harsh activation environment. This issue has been tackled by Zhang et al. [167] to prepare more stable adenine-based PCN-530 structure. Lin et al. have observed high density of open nitrogen-donor sites on 1,3,5-tris(2H-tetrazol-5-yl)benzene (H3BTT) which was responsible for the enhanced CO₂ capacity [146] through the improvement of the framework porosity and the utilization of nitrogen sites readily available to adsorb CO₂. However, the richness of nitrogen atoms in the framework does not necessarily favor CO₂ adsorption, as reported by Gao et al. [110] for the case of tetrazolate-based rth-MOF that has more exposed nitrogen sites as compared to pyrazolate-based rht-MOF and yet was showing less CO₂ uptake attributed to the strong electric field observed on the pyrazolate-based rht-MOF.

Other ligand modifications are also reported in literature by deploying several types of functional groups such as hydroxyl groups (OH) on Zn(BDC) [168], (CH₃)₂, (OH), and (COOH) on MIL-53(Al) [145], NO₂ on IRMOF-8 [107] as well as alkyl and nitro groups grafted on DUT-5 [169]. Based on the contribution by Yaghi's group [170], several studies were dedicated to understand the effects of ligand extension on the pore size, surface area, and the sorption behavior of MOFs [98, 109, 133, 171–173]. Recently, zeolite-like MOFs denoted as ZTIFs have attracted great interest due to their unique characteristics for tuning the structure toward various applications [174, 175]. New frameworks (ZTIF-1 and ZTIF-2) were recently reported based on the incorporation of tetrazolates into Zn-Imidazolate structures [176], with similar structures. UTSA-49 was also reported by Chen and coworkers for the selective separation of CO₂/N₂ mixture [117].

Lately, the idea of mixed ligand approach for the synthesis of MOFs with tunable properties has gained much attention which allows for incorporating several functionalities within each ligand to target certain properties such as improving the stability and the capacity for CO₂ simultaneously [177]. For instance, the water stability issue was tackled by Marco and coworkers [178] by utilizing two heterocyclic N-donor-mixed phosphonate-based organic ligands. The designed MOF has shown great water stability and achieved CO₂ uptake of 77 cm³/g at low pressure and 195 K. By deploying the mixed-ligand approach, Liu et al. [179] have successfully prepared Co-based MOFs containing both benzenetricarboxylic- and triazole-based ligands by using a solvo-thermal synthesis technique. The synthesized MOFs displayed CO₂ uptake of up to 15.2 wt. % at 1 bar and 295 K as well as remarkable selectivity toward nitrogen. A detailed investigation of mixed ligand approach in the design of MOFs is available in literature [180, 181]; however, further work is still needed to optimize the synthesis conditions and correlate the observed performance to the appropriate constituents on the organic

ligands. Recent work by Yaghi et al. provided tools to quantitatively map different functional groups incorporated into the same MOF structure [182].

3.2.3. Post-synthetic Functionalization of MOFs

As mentioned previously, tuning the affinity of the framework functionalities toward CO₂ is crucial for improving adsorptive capacities. The aim is to decorate the pore surface in order to have high adsorption selectivity and capacity and yet minimize the regeneration energy. In addition to the pre-synthetic modification of the organic linker, post-synthetic functionalization of MOFs (PSM) is considered a viable route to insert functionalities into the MOF structure after the formation of the basic framework. This approach can overcome the limitations observed in pre-synthetic functionalization, for instance precise control of the synthesis conditions is needed to preserve the functional groups during the solvo-thermal synthesis conditions. Note that some functional groups are not stable under synthesis conditions which require a narrow range of conditions to prepare the MOFs. Others, however, cannot be introduced to the synthesis mixture due to solubility issues, hindrance effects, and they might participate in the crystallization process and yield unwanted materials. Besides, inserting functional groups on the metal sites prior to the synthesis of the framework might intervene in the formation of the building units which can result in the deterioration of the crystal structure [183–185]. PSM is therefore considered an attractive pathway to tailor the properties of MOFs toward better CO₂ capture performance.

In order to make use of high amine affinity toward CO₂, several amine moieties were selected for the modification of various solid sorbents [186–189] including MOFs [190, 191]. Ethylene diamine (en) is considered the most commonly used type of amine for PSM of MOFs for CO₂ capture application. In 2014, Lee et al. [192] reported grafting the diamine into the expanded MOF-74 or Mg(dopbdc) structure at amine loadings of 16.7 wt. % at room temperature which exhibited very high CO₂ uptake of 13.7 wt% at 0.15 bar higher than the 12.1 wt. % capacity reported by McDonald et al. for N,N'-dimethylethylenediamine (mmen) grafted on Mg(dopbdc) [173]. The isosteric heat of adsorption was recorded to be 49 to 51 kJ/mol indicating chemisorption of CO₂ molecules which was further confirmed by the formation of carbamic acid probed by the in situ Fourier transform infrared spectroscopy (FTIR) experiments. The en grafted Mg(dopbdc) was further evaluated for the multicycle adsorption, and it has only lost 3% of its CO₂ uptake after five cycles. Moreover, en-Mg(dopbdc) has also shown stable structure and capacity after exposure to different moisture contents, and therefore this material has a potential for large-scale CO₂ capture (see Figure 5). NH₂, CH₂NH₂, CH₂NHMe along with other functional groups were recently grafted on IRMOF-74, and it was found that IRMOF-74-III-CH₂NH₂ displayed CO₂ capacity of 3.2 mmol/g at 1 bar [132]. The sodalite-type structure Cu-BTtri was also grafted by en functional group [193] which showed chemisorption interaction with the adsorbed CO₂ molecule as can be observed from the high isosteric heat of adsorption (90 kJ/mol). However, the en-Cu-BTtri has only shown improved capacity at low pressure while the unmodified MOF shows higher uptakes at high pressure which is attributed to the significant reduction in Brunauer–Emmett–Teller (BET) surface area from 1770 to 345 m²/g due to the pore blocking effect of the en

group. In an attempt to address this issue, McDonald et al. functionalized mmen group on Cu-BTTRI and preserved a BET surface area of 870 m²/g with 96 kJ/mol isosteric heat of adsorption, nitrogen selectivity of 327, and CO₂ uptake of 9.5 wt.% under 0.15 bar CO₂/0.75 bar N₂ mixture at 25 °C. The negative impact of alkylamine functional groups on reducing the surface area was evident, and one approach to overcome this issue is to introduce ligand extension prior to the introduction of the amine group so as to increase the MOF porosity and avoid the pore-blocking problem during PSMs [132]. Also, a deep insight into the mechanism of CO₂ adsorption on alkylamine-grafted MOFs is crucial to further understand the interactions for improved structural design and amine loadings [194]. Other amine functionalities such as piperazine were also grafted into Cu-BTTRI [128] and exhibited 2.5 times higher CO₂ uptake as compared to bare Cu-BTTRI, while the heat of adsorption confirms the chemisorption interactions. The area reduction was also evident as it was reduced from 1700 m²/g to 380 m²/g (similar to ethylenediamine, (en)- Cu-BTTRI [195]). Pyridine was also grafted on Ni-DOBDC to improve the water stability and increase the hydrophobicity of the material [196]. Experimental observations supported by simulation results confirmed the enhanced water stability for the Pyridine-Ni-DOBDC samples while maintaining the CO₂ uptake at atmospheric conditions and low pressures. It was also concluded that the amine moiety was grafted on the unsaturated metal sites of the framework, which makes this approach desirable for amine functionalization. From a combined experimental and simulation study, it was found that pyridine modification of an MOF can reduce H₂O adsorption while retaining considerable CO₂ capacity at conditions of interest for flue gas separation. This indicates that post-synthesis modification of MOFs by coordinating hydrophobic ligands to unsaturated metal sites may be a powerful method to generate new sorbents for gas separation under humid conditions. Amine functionalization to target the water stability of MOFs will be further discussed in the next section.

It is evident from the previous discussion that amine impregnation into MOFs always sacrifices the surface area of the final product. Therefore, the choice of the amine that can improve the affinity toward CO₂ and attain high surface area simultaneously is a trade-off issue. MIL-101 materials were reported to have the highest pore volume and surface area among MOFs to date (BET = 3125 m²/g and 1.63 cm³/g). Hence they allow the incorporation of amines with longer alkyl chains such as polyethyleneimine while at the same time maintaining relatively high surface area (1112.6 m²/g after 75 wt% amine loading). PEI-loaded MIL-101 prepared by Lin et al. [197] exhibited remarkably high CO₂ uptake of 4.2 mmol/g at 0.15 bar and 298 K with exceptional CO₂/N₂ selectivity of 770 at 25 °C.

Optimization of amine loadings and distribution within the MOF structure is a detrimental factor for the impact of these functionalities on the performance in CO₂ capture process. Precise control of the different factors during the grafting process is crucial to append these groups exactly on the unsaturated metal centers, while avoid blocking the pores and hindering access to the interior volume. Improving the PSM methods is considered one of the means to achieve the ideal grafting and amine distribution [191].

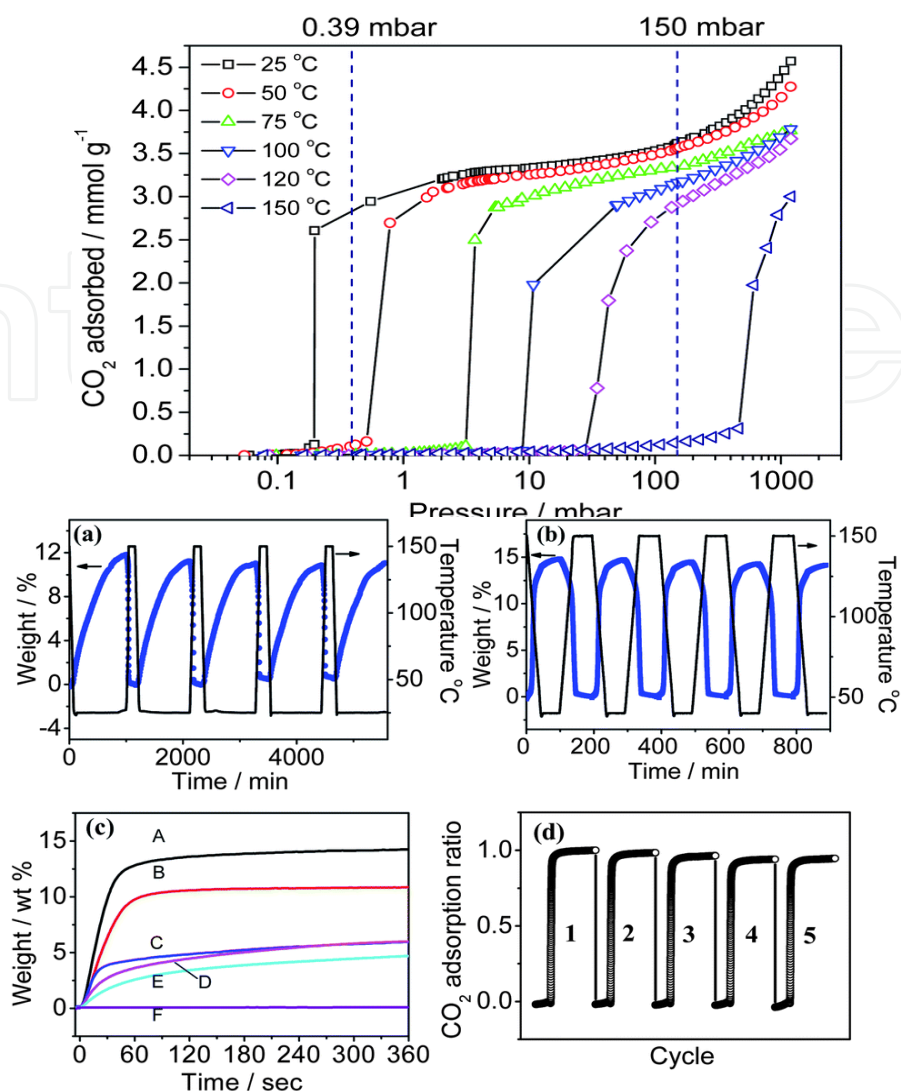


Figure 5. Top: Adsorption isotherms of CO₂ for 1-en at the indicated temperatures. Bottom: Adsorption–desorption cycling of CO₂ for 1-en showing reversible uptake from (a) simulated air (0.39 mbar CO₂ and 21% O₂ balanced with N₂) and from (b) simulated flue gas (0.15 bar CO₂ balanced with N₂). (c) time-dependent CO₂ adsorption for porous materials (A = 1-en, B = mmen-Mg₂(dobpdc), C = 1, D = Mg-MOF-74, E = Zeolite 13X, F = MOF-5). (d) CO₂ adsorption ratio of 1-en in flue gas (after 6 min exposure to 100% RH at 21 °C) to 1-en in flue gas (Adapted from [192]).

4. Recent Advances and Current Trends

4.1. Hybrid Systems Based on MOFs

For more efficient utilization of MOFs sorbents, several hybrid systems based on MOFs with other solid sorbents have been investigated in the literature. The objective of having hybrid materials is to utilize the synergism between the two sorbents and therefore ultimately improve the overall performance in CO₂ separation. Moreover, sorbents such as activated carbons, graphenes, and CNTs provide the added feature of high surface area and easily functionalized sites which contribute to the tuning of the final properties of the composite

material. CNTs represent one of the effective candidates that can improve the properties of MOFs for gas adsorption applications. Zhu et al. [198] incorporated HKUST-1 in the interspace of CNTs. The designed composite exhibited superior selectivity and a CO₂ saturation capacity of 7.83 mmol/g at 298 K, which was attributed to the high porosity and surface area. In a similar study, multiwall CNTs, well dispersed in MIL-101 (Cr), were successfully prepared and maintained the same framework and crystal structure as MIL-101. An increase of 60% in CO₂ uptake was observed for the MWCNT-MIL-101 composite which was attributed to the increased porosity as a result of incorporating CNTs [199], as was confirmed by similar work on MWCNT-MIL-53(Cu) composite [200].

Graphene oxide composites with different MOFs are extensively reported in the literature such as HKUST-1 [201], MOF-5 [202], and Cu-BTC [203]. Graphite oxide (GO) is considered a stabilizing agent for MOFs under humid environment, and it has shown remarkable CO₂ capacity of 3.3 mmol/g and great stability under simulated flue gas conditions for GO/Cu-BTC composite [203]. The synthesis of Cu-based MOFs composite with aminated graphite oxides (GO) was carried out and fully characterized by Zhao et al. [204]. The composite exhibited 50% enhanced porosity as compared to the parent MOF and displayed unique structure and pore sizes effective for size exclusion separation of CO₂ from the flue gas. Silica aerogel (SA) was also investigated as a promising candidate for hybrid systems with ZIF-8 [205]. The detailed characterizations of the SA/ZIF-8 confirmed the presence of the two phases in the composite after sol-gel synthesis procedure with different ZIF-8 loadings and mild BET surface area [205].

Several composite materials have been reported for various applications; however, utilizing these hybrid systems in CO₂ adsorption might be a promising route for improving the CO₂ capture process. Ahmed et al. [206] published a review of information related to the synthesis and adsorption applications of MOF composite materials.

4.2. Ionic Liquids/MOF Composites

Ionic liquids as solvents for the absorption separation of CO₂ from flue gas are discussed in Section 1.2 in order to overcome the limitations related to the poor dynamics of CO₂ separation in ILs due to their high viscosity. MOFs can act as an ideal support material for the incorporation of ILs into their porous structure while preserving their unique properties. The concept of immobilization of ILs into solid sorbents has been reported for various applications. For instance, ILs immobilization on mesoporous silica was reported for the catalytic esterification reaction [207], ILs addition into polymer gels for ionic conductivity applications [208], ILs/Zeolite composites [209], in addition to several review papers available on this topic indicating the widespread use of this new approach over the past years [210, 211]. Computational investigation of the theoretical possibility of incorporating ILs into MOFs was studied by Jiang's group for (BMIM)PF₆ IL supported on IRMOF-1 for CO₂ capture applications [212]. The confinement effects of the narrow pore on the ILs and the ionic interactions between [BMIM]⁺ favor the open pore while the anion, [PF₆]⁻, was attached to the open metal sites, was observed in a simulation study. It was ascertained that CO₂ was favorably attached to the [PF₆]⁻ anions sites. The study demonstrated that IL/MOF composites are a potential candidate for CO₂ adsorption and have displayed significantly high CO₂/N₂ selectivity. To the best of our

knowledge, the first report on an experimental attempt to immobilize ILs into MOF structures was published by Liu et al. [213] for the insertion of Bronsted acidic ILs (BAIL) into the pores of MIL-101 using post-synthetic approach with triethylene diamine (TEDA) or imidazole (IMIZ) as a solvent assisting during the functionalization process. Nitrogen adsorption isotherms of bare MIL-101, TEDA-BAIL/MIL-101, and all (IMIZ-BAIL/MIL-101) samples showed type-I isotherm indicating the microporous nature of the composite. BET surface area was 1873 m²/g for the bare MIL-101 which was slightly decreased to 1728 m²/g and 1148 m²/g for IMIZ-BAIL/MIL-101 and TEDA-BAIL/MIL-101, respectively. Following this leading report, Jhung's group [214] successfully grafted up to 50 wt.% acidic chloroaluminate IL on MIL-101 which reduced the BET surface area of the bare MIL-101 by around 60%. The incorporation of ILs with basic nature which is favorable for CO₂ adsorption was for the first time reported by Kitagawa et al. [215]. A detailed characterization and investigation of the phase behavior of the immobilized 1-ethyl-3-methylimidazolium bis(trifluoromethylsulfonylamide) denoted as EMI-TFSA ILs into ZIF-8 was presented in this study. A reduction of 29% in pore volume was measured in N₂ adsorption isotherm experiments and computational calculations. The EMI-TFSA/ZIF-8 composite has shown distinctive ion conductivity at low temperature as reported in a second paper by the same group [216]. The prospect of IL/MOF composite for gas separation is still under computational investigation with no reported experimental studies of CO₂ adsorption on these composites. Recently, Vincent-Luna et al. [15] investigated the effects of adding room temperature ILs (RTILs) into the pores of Cu-BTC structures. The adsorption of CO₂, N₂, CH₄, and their mixtures were studied by utilizing various RTILs having the same cation 1-ethyl-3-methylimidazolium [EMIM]⁺ and different anions such as bis[(trifluoromethyl)-sulfonyl]imide [Tf₂N]⁻, thiocyanate [SCN]⁻, nitrate [NO₃]⁻, tetrafluoroborate [BF₄]⁻, and hexafluorophosphate [PF₆]⁻. The RTIL/Cu-BTC composite has shown enhanced CO₂ uptakes at low pressures with high CO₂/N₂ selectivity due to the polarization driving force rendering these materials as a promising system for post-combustion CO₂ capture. Another application of IL/MOF composite as a precursor for the preparation of nitrogen and boron–nitrogen (N- and BN-)-decorated porous carbons was recently reported by Aijaz et al. [217] as a novel synthesis strategy.

4.3. Ab/Adsorption in Ionic Liquids/MOF Slurry System

Another approach to utilize the combined synergistic advantages of MOF and IL composites is through a novel hybrid adsorption–absorption technology. This novel technology can provide an efficient approach to utilize the high capacity, selectivity, and low heat of adsorption of the solid sorbents along with the advantages of having a continuous flow process that allows for better heat integration and separation rates in contrast to the conventional batch process used in adsorption-only process. Mass transfer enhancement due to the dispersion of fine solids in liquid solvents was studied and insight into the mechanism and the analysis of different mass transfer resistances were described by Zhang and coworkers [218] which was in agreement with previous findings [219–221]. As far as enhancement of CO₂ capture in slurry systems is concerned, a study dealing with AC particles dispersed in K₂CO₃ aqueous solution was reported by Sumin et al. [222] to investigate the influence of the hydrodynamics on the mass transfer improvements. In a similar work by Rosu et al. [223], AC particles were also

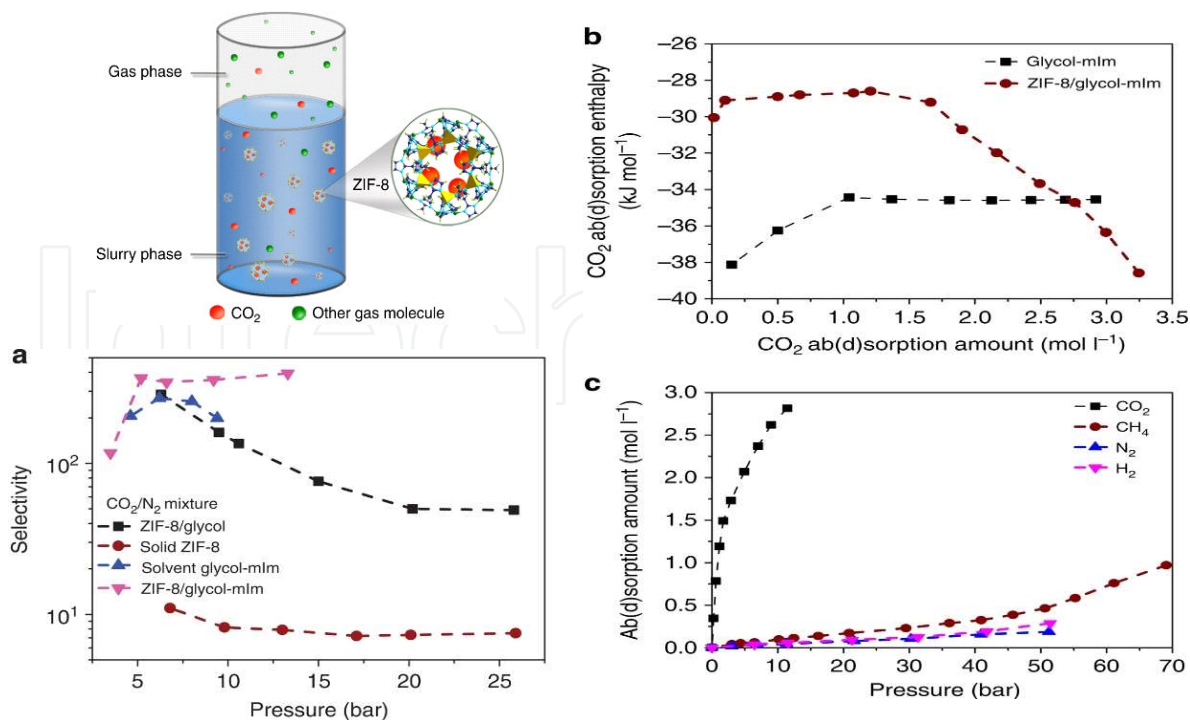


Figure 6. Top left: schematic of the slurry system. (a) Comparison of selectivity toward N₂ (b) ab/adsorption enthalpy. (c) CO₂ uptake at 303.15 K (Adapted from [225]).

found to improve the absorptive CO₂ capture process. The unique characteristics of MOFs in CO₂ adsorption and their recent applications in aqueous solution environment [224] have opened the door toward the possibility of immersing MOF particles in various physical and chemical solvents for CO₂ separation application. This novel unit operation process can overcome the limitations reported for conventional adsorption on MOFs such as high pressure drop and the necessity for formulating the powders into different shapes and sizes which affects their structural stability and reduces the active surface area. Liu et al. [225] reported, for the first time, the preparation of ZIF-8/glycol and ZIF-8/glycol/2-methylimidazole slurries (Figure 6). CO₂ uptake of 1.25 mmol/L was recorded for the slurry system with CO₂/N₂ selectivity of 394 at 1 bar, and most importantly a very low enthalpy of 29 kJ/mol. In a similar work by Lei et al. [226], ILs [EMIM, TF2N] and [OMIM, PF6] were used to prepare slurry systems with ZIF-8 and ZIF-7. CO₂ adsorption in the slurry system has shown a promising performance with isosteric heat of adsorption less than 26 kJ/mol. Following these two studies, the solubility of CO₂ in physical solvents such as methanol mixed with ZIF-8 was also investigated [227]. The study revealed that ZIF-8 can significantly improve the low pressure-CO₂ uptake in physical solvents and can dramatically reduce the solvent losses by evaporation to the gas phase at the top of the absorber. Increasing ZIF-8 loadings has shown further enhancement of the CO₂ capacity, as observed previously [225]; however, it is worth noting that a high solid loading in the slurry system was not recommended from process engineering point of view as it might cause some problems during the pumping of the slurry mixture and increases the solid losses in the multicycle separation process [225].

For future studies on MOF-based slurry systems, there is basic selection of criteria that needs to be satisfied by both MOF and the liquid solution. The selection of the MOF possessing the appropriate pore size for the preparation of the slurry system is very important to guarantee that the size of the liquid is large enough and does not occupy the pores which leaves no space for CO₂ to adsorb. Moreover, the structural stability of the MOF in the aqueous solution is essential so that it does not lose its porous framework nor its surface area. The selection of the liquid candidate is crucial, as it should not provide any extra mass transfer resistance for CO₂ molecules. Further, experimental and computational investigations are still required to understand the separation mechanism in slurry mixtures and to have insight into the different types of interactions between the gas, liquid, and solid materials.

5. Challenges and Outlook

In conclusion, MOFs are considered the largest growing research area in CO₂ capture, with great achievements and developments. Due to their versatile structures and possibilities for various functionalization approaches, the door is still open for further improvements and advancements of their performance under real flue gas conditions, and in large-scale applications. Although we have reported MOFs with distinguished properties and exceptional CO₂ capacity, selectivity, and stability, there are still some concerns that need to be addressed before reaching commercial scale level. The lack of information about the performance of MOFs under real gas mixture conditions is one of the key issues to understand the actual working uptakes and identify any possible limitations. Further experimental testing of MOFs using, for example, a gas mixture containing all the impurities that might be present in an actual flue gas is needed high-throughput technique. Computational gas mixture studies can provide essential information in this regard; however, experimental investigation is still considered the most reliable approach. MOF stabilities in humid conditions, high temperature, and harsh mechanical stress situations must be given much attention. Several studies were performed to target MOF stability, and great achievements were recorded in this field [228, 229], as reviewed in references [160, 230]. Finally, in the following section, we focus on water stability studies as it is one of the main drawbacks of MOFs.

5.1. Water Stability of MOFs

Water stability is a major challenge that has to be overcome before metal organic framework can be used in removing carbon dioxide from flue gas. The core structure of MOF reacts with water vapor content in the flue gas leading to severe distortion of the structure and even failure. As a consequence, the physical structure of MOF is changed, e.g., reduction of porosity and surface area, etc. that decreases the capacity and selectivity for CO₂. Complete dehydration of flue gas increases the cost of separation. It is therefore essential for MOFs to exhibit stability in the presence of water up to certain extent [91].

Metal–ligand coordination bond, which is the most significant part of MOF, is hydrolyzed with water, resulting in the displacement of ligand bond; and as a consequence, the whole structure

usually collapses [91]. The stability of MOF in the presence of water depends on the strength of metal ligand bond. pK_a values of the ligand atom can be considered as the strength of this metal- ligand bond. Since the hydrolysis reaction between MOF and water molecule is governed by Gibbs free energy and activation energy of the reactant and product molecules, thermodynamics and kinetics factors have great influence on the water stability of MOF [160]. Insight into the molecular structure, more specifically the metal–ligand strength, the weakest part of MOF, and thermodynamics as well as kinetics study of hydrolysis reaction are very important to improve water stability. Several strategies based on these two important aspects have been taken into consideration.

Jasuja et al. [231] performed a study on the effects of functionalization of the organic ligand in a series of isostructural MOFs in the Zn(BDC-X)-(DABCO)0.5 family on water stability. In this experiment, they cyclically stabilized an unstable parent structure in humid conditions through the incorporation of tetramethyl-BDC ligand. The results of molecular simulation disclosed that the kinetic stability is improved due to the carboxylate oxygen in the DMOF-TM2 structure which acted as a shield to prevent hydrogen-bonding interactions and subsequent structural transformations. Hence, electrophilic zinc atoms in this structure became inaccessible to the nucleophilic oxygen atoms in water, resulting in prevention of the hydrolysis reactions for the displacement ligand. They also performed another study to evaluate the effect of strength of metal–ligand coordination bond and catenation in the framework on water stability [232]. According to their results, the non-interpenetrated MOFs constructed from a pillar ligand of higher pK_a exhibited higher stability; however, interpenetrated MOFs constructed from a pillar ligand of lower pK_a values exhibited less stability. The interpenetration in MOF with incorporation of ligands of relatively high basicity exhibited good water stability. By considering the results of previous experiment, they synthesized cobalt-, nickel-, copper-, and zinc-based, new pillared MOFs of similar topologies which exhibited good water stability [233]. The grafted methyl group on the benzene dicarboxylate (BDC) ligand introduced steric factors around the metal centers; consequently, water stability of MOF drastically improved. The basicity of BTTB-based MOFs synthesized with bipyridyl pillar ligands had lower basicity than DABCO; however, they exhibited better stability in the presence of humid condition.

Bae et al. [114] performed a study to modify Ni-DOBDC with pyridine molecules. The study showed that pyridine molecule made the normally hydrophilic internal surface more hydrophobic; as a result, water absorption was reduced, while substantial CO₂ capture capacity was retained to a certain level. Fracaroli et al. [132] improved the interior of IRMOF-74-III by covalently functionalizing it with a primary amine, and used a MOF, IRMOF-74-III-CH₂NH₂, for the selective capture of CO₂ in 65% relative humidity.

Zhang et al. [234] performed a study to modify the surface of the MOF hydrophilic to hydrophobic to improve water stability. They demonstrated a new strategy to modify hydrophobic polydimethylsiloxane (PDMS) on the surface to significantly enhance their water resistance by a facile vapor deposition technique. In this study, they successfully coated three vulnerable MOFs according to the water stability (MOF-5, HKUST-1, and ZnBT), while the porosity, crystalline characteristics, and surface area were unchanged.

All these studies demonstrated that water stability of MOFs can be improved by incorporating specific factors (e.g., metal–ligand strength, thermodynamic and kinetic factors, etc.) which govern the structural stability of the framework.

Author details

Mohanned Mohamedali, Devjyoti Nath, Hussameldin Ibrahim and Amr Henni*

*Address all correspondence to: amr.henni@uregina.ca

Industrial/Process Systems Engineering, Faculty of Engineering and Applied Science,
University of Regina, Regina, SK, Canada

References

- [1] World Meteorological Organization, *WMO Greenhouse Gas Bulletin No. 10*, Geneva, Switzerland 2014.
- [2] Energy Information Administration (EIA), *Annual Energy Outlook*, Washington, United States, 2014.
- [3] A. A. Olajire, *Energy*, 2010, 35, 2610–2628.
- [4] J. D. Figueroa, T. Fout, S. Plasynski, H. McIlvried and R. D. Srivastava, *International Journal of Greenhouse Gas Control*, 2008, 2, 9–20.
- [5] M. Wang, A. Lawal, P. Stephenson, J. Sidders and C. Ramshaw, *Chemical Engineering Research and Design*, 2011, 89, 1609–1624.
- [6] G. Puxty, R. Rowland, A. Allport, Q. Yang, M. Bown, R. Burns, M. Maeder and M. Attalla, *Environmental Science & Technology*, 2009, 43, 6427–6433.
- [7] C.-H. Yu, C.-H. Huang and C.-S. Tan, *Aerosol and Air Quality Research*, 2012, 12, 745–769.
- [8] R. Idem, M. Wilson, P. Tontiwachwuthikul, A. Chakma, A. Veawab, A. Aroonwilas and D. Gelowitz, *Industrial & Engineering Chemistry Research*, 2006, 45, 2414–2420.
- [9] G. T. Rochelle, *Science*, 2009, 325, 1652–1654.
- [10] S. Rackley, *Carbon Capture and Storage*, Gulf Professional Publishing, Houston, USA 2009.
- [11] Q. Zhuang, R. Pomalis, L. Zheng and B. Clements, *Energy Procedia*, 2011, 4, 1459–1470.

- [12] Z. Lei, C. Dai and B. Chen, *Chemical Reviews*, 2013, 114, 1289–1326.
- [13] M. Ramdin, A. Amplianitis, S. Bazhenov, A. Volkov, V. Volkov, T. J. Vlugt and T. W. de Loos, *Industrial & Engineering Chemistry Research*, 2014, 53, 15427–15435.
- [14] J. F. Brennecke and B. E. Gurkan, *The Journal of Physical Chemistry Letters*, 2010, 1, 3459–3464.
- [15] J. M. Vicent-Luna, J. J. Gutiérrez-Sevillano, J. A. Anta and S. Calero, *The Journal of Physical Chemistry C*, 2013, 117, 20762–20768.
- [16] L. Zhou, J. Fan and X. Shang, *Materials*, 2014, 7, 3867–3880.
- [17] R. D. Rogers and K. R. Seddon, *Science*, 2003, 302, 792–793.
- [18] M. Ramdin, T. W. de Loos and T. J. Vlugt, *Industrial & Engineering Chemistry Research*, 2012, 51, 8149–8177.
- [19] E. D. Bates, R. D. Mayton, I. Ntai and J. H. Davis, *Journal of the American Chemical Society*, 2002, 124, 926–927.
- [20] Z.-Z. Yang, Y.-N. Zhao and L.-N. He, *RSC Advances*, 2011, 1, 545–567.
- [21] H. G. Joglekar, I. Rahman and B. D. Kulkarni, *Chemical Engineering & Technology*, 2007, 30, 819–828.
- [22] J.-R. Li, Y. Ma, M. C. McCarthy, J. Sculley, J. Yu, H.-K. Jeong, P. B. Balbuena and H.-C. Zhou, *Coordination Chemistry Reviews*, 2011, 255, 1791–1823.
- [23] A. W. Chester and E. G. Derouane, *Zeolite characterization and catalysis*, Springer, 2009.
- [24] A. Primo and H. Garcia, *Chemical Society Reviews*, 2014, 43, 7548–7561.
- [25] T. F. Degnan Jr, *Topics in Catalysis*, 2000, 13, 349–356.
- [26] W. Hölderich, J. Röseler, G. Heitmann and A. Liebens, *Catalysis Today*, 1997, 37, 353–366.
- [27] M. Davis, *Microporous and Mesoporous Materials*, 1998, 21, 173–182.
- [28] S. Cavenati, C. A. Grande and A. E. Rodrigues, *Energy & Fuels*, 2006, 20, 2648–2659.
- [29] S. Himeno, T. Tomita, K. Suzuki and S. Yoshida, *Microporous and Mesoporous Materials*, 2007, 98, 62–69.
- [30] R. V. Siriwardane, M.-S. Shen, E. P. Fisher and J. A. Poston, *Energy & Fuels*, 2001, 15, 279–284.
- [31] R. V. Siriwardane, M.-S. Shen and E. P. Fisher, *Energy & Fuels*, 2003, 17, 571–576.
- [32] J. Merel, M. Clause and F. Meunier, *Industrial & Engineering Chemistry Research*, 2008, 47, 209–215.

- [33] T. Remy, S. A. Peter, L. Van Tendeloo, S. Van der Perre, Y. Lorgouilloux, C. E. Kirschhock, G. V. Baron and J. F. Denayer, *Langmuir*, 2013, 29, 4998–5012.
- [34] J. Shang, G. Li, R. Singh, P. Xiao, J. Z. Liu and P. A. Webley, *The Journal of Physical Chemistry C*, 2013, 117, 12841–12847.
- [35] F. Su and C. Lu, *Energy & Environmental Science*, 2012, 5, 9021–9027.
- [36] S.-H. Hong, M.-S. Jang, S. J. Cho and W.-S. Ahn, *Chemical Communications*, 2014, 50, 4927–4930.
- [37] O. Cheung, Z. Bacsik, Q. Liu, A. Mace and N. Hedin, *Applied Energy*, 2013, 112, 1326–1336.
- [38] A. Goj, D. S. Sholl, E. D. Akten and D. Kohen, *The Journal of Physical Chemistry B*, 2002, 106, 8367–8375.
- [39] S. Loganathan, M. Tikmani and A. K. Ghoshal, *Langmuir*, 2013, 29, 3491–3499.
- [40] C. F. Cogswell, H. Jiang, J. Ramberger, D. Accetta, R. J. Willey and S. Choi, *Langmuir*, 2015, 31, 4534–4541.
- [41] R. Veneman, H. Kamphuis and D. Brilman, *Energy Procedia*, 2013, 37, 2100–2108.
- [42] D. P. Bezerra, R. S. Oliveira, R. S. Vieira, C. L. Cavalcante Jr and D. C. Azevedo, *Adsorption*, 2011, 17, 235–246.
- [43] S. C. Lee, C. C. Hsieh, C. H. Chen and Y. S. Chen, *Aerosol and Air Quality Research*, 2013, 13, 360–366.
- [44] Y. Jing, L. Wei, Y. Wang and Y. Yu, *Microporous and Mesoporous Materials*, 2014, 183, 124–133.
- [45] Y.-K. Kim, Y.-H. Mo, J. Lee, H.-S. You, C.-K. Yi, Y. C. Park and S.-E. Park, *Journal of Nanoscience and Nanotechnology*, 2013, 13, 2703–2707.
- [46] K. Ahmad, O. Mowla, E. M. Kennedy, B. Z. Dlugogorski, J. C. Mackie and M. Stockenhuber, *Energy Technology*, 2013, 1, 345–349.
- [47] C. H. Lee, D. H. Hyeon, H. Jung, W. Chung, D. H. Jo, D. K. Shin and S. H. Kim, *Journal of Industrial and Engineering Chemistry*, 2015, 23, 251–256.
- [48] J. Kim, L.-C. Lin, J. A. Swisher, M. Haranczyk and B. Smit, *Journal of the American Chemical Society*, 2012, 134, 18940–18943.
- [49] D. Marx, L. Joss, M. Hefti, R. Pini and M. Mazzotti, *Energy Procedia*, 2013, 37, 107–114.
- [50] G. Li, P. Xiao, P. Webley, J. Zhang, R. Singh and M. Marshall, *Adsorption*, 2008, 14, 415–422.
- [51] A. Sayari and Y. Belmabkhout, *Journal of the American Chemical Society*, 2010, 132, 6312–6314.

- [52] S. Esposito, A. Marocco, G. Dell'Agli, B. De Gennaro and M. Pansini, *Microporous and Mesoporous Materials*, 2015, 202, 36–43.
- [53] R. A. Fiuza Jr, R. Medeiros de Jesus Neto, L. B. Correia and H. M. Carvalho Andrade, *Journal of Environmental Management*, 2015, 161, 198–205.
- [54] E. David and J. Kopac, *Journal of Analytical and Applied Pyrolysis*, 2014, 110, 322–332.
- [55] F. Montagnaro, A. Silvestre-Albero, J. Silvestre-Albero, F. Rodríguez-Reinoso, A. Erto, A. Lancia and M. Balsamo, *Microporous and Mesoporous Materials*, 2015, 209, 157–164.
- [56] M. Kacem, M. Pellerano and A. Delebarre, *Fuel Processing Technology*, 2015, 138, 271–283.
- [57] D. Xu, P. Xiao, J. Zhang, G. Li, G. Xiao, P. A. Webley and Y. Zhai, *Chemical Engineering Journal*, 2013, 230, 64–72.
- [58] G. Sethia and A. Sayari, *Carbon*, 2015, 93, 68–80.
- [59] N. Díez, P. Álvarez, M. Granda, C. Blanco, R. Santamaría and R. Menéndez, *Chemical Engineering Journal*, 2015, 281, 704–712.
- [60] R.-L. Tseng, F.-C. Wu and R.-S. Juang, *Separation and Purification Technology*, 2015, 140, 53–60.
- [61] A. Houshmand, M. S. Shafeeyan, A. Arami-Niya and W. M. A. W. Daud, *Journal of the Taiwan Institute of Chemical Engineers*, 2013, 44, 774–779.
- [62] M. J. Mostazo-López, R. Ruiz-Rosas, E. Morallón and D. Cazorla-Amorós, *Carbon*, 2015, 91, 252–265.
- [63] J. A. A. Gibson, A. V. Gromov, S. Brandani and E. E. B. Campbell, *Microporous and Mesoporous Materials*, 2015, 208, 129–139.
- [64] M. S. Shafeeyan, W. M. A. W. Daud, A. Shamiri and N. Aghamohammadi, *Chemical Engineering Research and Design*, 2015, 104, 42–52.
- [65] Q. Liu, Y. Shi, S. Zheng, L. Ning, Q. Ye, M. Tao and Y. He, *Journal of Energy Chemistry*, 2014, 23, 111–118.
- [66] M.-S. Lee and S.-J. Park, *Journal of Solid State Chemistry*, 2015, 226, 17–23.
- [67] M.-S. Lee, S.-Y. Lee and S.-J. Park, *International Journal of Hydrogen Energy*, 2015, 40, 3415–3421.
- [68] F. Su, C. Lu, W. Cnen, H. Bai and J. F. Hwang, *Science of The Total Environment*, 2009, 407, 3017–3023.
- [69] A. Kumar Mishra and S. Ramaprabhu, *RSC Advances*, 2012, 2, 1746–1750.

- [70] M. M. Gui, Y. X. Yap, S.-P. Chai and A. R. Mohamed, *International Journal of Greenhouse Gas Control*, 2013, 14, 65–73.
- [71] Y. G. Ko, H. J. Lee, H. C. Oh and U. S. Choi, *Journal of Hazardous Materials*, 2013, 250–251, 53–60.
- [72] K. S. Novoselov, A. K. Geim, S. V. Morozov, D. Jiang, Y. Zhang, S. V. Dubonos, I. V. Grigorieva and A. A. Firsov, *Science*, 2004, 306, 666–669.
- [73] S.-M. Hong, S. H. Kim and K. B. Lee, *Energy & Fuels*, 2013, 27, 3358–3363.
- [74] M. Asai, T. Ohba, T. Iwanaga, H. Kanoh, M. Endo, J. Campos-Delgado, M. Terrones, K. Nakai and K. Kaneko, *Journal of the American Chemical Society*, 2011, 133, 14880–14883.
- [75] L.-Y. Meng and S.-J. Park, *Journal of Colloid and Interface Science*, 2012, 386, 285–290.
- [76] F. Li, X. Jiang, J. Zhao and S. Zhang, *Nano Energy*, 2015, 16, 488–515.
- [77] S. Gadipelli and Z. X. Guo, *Progress in Materials Science*, 2015, 69, 1–60.
- [78] A. Taheri Najafabadi, *Renewable and Sustainable Energy Reviews*, 2015, 41, 1515–1545.
- [79] K. C. Kemp, V. Chandra, M. Saleh and K. S. Kim, *Nanotechnology*, 2013, 24, 235703.
- [80] J. Oh, Y.-H. Mo, V.-D. Le, S. Lee, J. Han, G. Park, Y.-H. Kim, S.-E. Park and S. Park, *Carbon*, 2014, 79, 450–456.
- [81] W. Li, X. Jiang, H. Yang and Q. Liu, *Applied Surface Science*, 2015, 356, 812–816.
- [82] S. Chowdhury, G. K. Parshetti and R. Balasubramanian, *Chemical Engineering Journal*, 2015, 263, 374–384.
- [83] J. Wang, X. Mei, L. Huang, Q. Zheng, Y. Qiao, K. Zang, S. Mao, R. Yang, Z. Zhang, Y. Gao, Z. Guo, Z. Huang and Q. Wang, *Journal of Energy Chemistry*, 2015, 24, 127–137.
- [84] Y. Zhao, H. Ding and Q. Zhong, *Applied Surface Science*, 2013, 284, 138–144.
- [85] Y. Cao, Y. Zhao, Z. Lv, F. Song and Q. Zhong, *Journal of Industrial and Engineering Chemistry*, 2015, 27, 102–107.
- [86] S. Pourebrahimi, M. Kazemeini, E. Ganji Babakhani and A. Taheri, *Microporous and Mesoporous Materials*, 2015, 218, 144–152.
- [87] J.-R. Li, R. J. Kuppler and H.-C. Zhou, *Chemical Society Reviews*, 2009, 38, 1477–1504.
- [88] T. Duren, Y.-S. Bae and R. Q. Snurr, *Chemical Society Reviews*, 2009, 38, 1237–1247.
- [89] S. Kitagawa, R. Kitaura and S.-i. Noro, *Angewandte Chemie International Edition*, 2004, 43, 2334–2375.
- [90] O. M. Yaghi, M. O’Keeffe, N. W. Ockwig, H. K. Chae, M. Eddaoudi and J. Kim, *Nature*, 2003, 423, 705–714.

- [91] K. Sumida, D. L. Rogow, J. A. Mason, T. M. McDonald, E. D. Bloch, Z. R. Herm, T.-H. Bae and J. R. Long, *Chemical reviews*, 2011, 112, 724–781.
- [92] K. C. Stylianou and W. L. Queen, *CHIMIA International Journal for Chemistry*, 2015, 69, 274–283.
- [93] Z. Zhang, Z.-Z. Yao, S. Xiang and B. Chen, *Energy & Environmental Science*, 2014, 7, 2868–2899.
- [94] J. Wang, L. Huang, R. Yang, Z. Zhang, J. Wu, Y. Gao, Q. Wang, D. O'Hare and Z. Zhong, *Energy & Environmental Science*, 2014, 7, 3478–3518.
- [95] J.-R. Li, J. Sculley and H.-C. Zhou, *Chemical Reviews*, 2011, 112, 869–932.
- [96] J.-R. Li, R. J. Kuppler and H.-C. Zhou, *Chemical Society Reviews*, 2009, 38, 1477–1504.
- [97] L. Li, S. Tang, C. Wang, X. Lv, M. Jiang, H. Wu and X. Zhao, *Chemical Communications*, 2014, 50, 2304–2307.
- [98] J. Cai, X. Rao, Y. He, J. Yu, C. Wu, W. Zhou, T. Yildirim, B. Chen and G. Qian, *Chemical Communications*, 2014, 50, 1552–1554.
- [99] M. Taddei, F. Costantino, F. Marmottini, A. Comotti, P. Sozzani and R. Vivani, *Chemical Communications*, 2014, 50, 14831–14834.
- [100] M. Taddei, F. Costantino, A. Ienco, A. Comotti, P. V. Dau and S. M. Cohen, *Chemical Communications*, 2013, 49, 1315–1317.
- [101] Y. Peng, G. Srinivas, C. E. Wilmer, I. Eryazici, R. Q. Snurr, J. T. Hupp, T. Yildirim and O. K. Farha, *Chemical Communications*, 2013, 49, 2992–2994.
- [102] J. Kim, Y.-R. Lee and W.-S. Ahn, *Chemical Communications*, 2013, 49, 7647–7649.
- [103] Y. He, H. Furukawa, C. Wu, M. O'Keeffe, R. Krishna and B. Chen, *Chemical Communications*, 2013, 49, 6773–6775.
- [104] X. Wu, M. N. Shahrak, B. Yuan and S. Deng, *Microporous and Mesoporous Materials*, 2014, 190, 189–196.
- [105] G. Yang, J. A. Santana, M. E. Rivera-Ramos, O. García-Ricard, J. J. Saavedra-Arias, Y. Ishikawa, A. J. Hernández-Maldonado and R. G. Raptis, *Microporous and Mesoporous Materials*, 2014, 183, 62–68.
- [106] E. Deniz, F. Karadas, H. A. Patel, S. Aparicio, C. T. Yavuz and M. Atilhan, *Microporous and Mesoporous Materials*, 2013, 175, 34–42.
- [107] S. Orefuwa, E. Iriowen, H. Yang, B. Wakefield and A. Goudy, *Microporous and Mesoporous Materials*, 2013, 177, 82–90.
- [108] S. Ye, X. Jiang, L.-W. Ruan, B. Liu, Y.-M. Wang, J.-F. Zhu and L.-G. Qiu, *Microporous and Mesoporous Materials*, 2013, 179, 191–197.

- [109] N. C. Burtch, H. Jasuja, D. Dubbeldam and K. S. Walton, *Journal of the American Chemical Society*, 2013, 135, 7172–7180.
- [110] W.-Y. Gao, T. Pham, K. A. Forrest, B. Space, L. Wojtas, Y.-S. Chen and S. Ma, *Chemical Communications*, 2015, 51, 9636–9639.
- [111] D. Wang, B. Liu, S. Yao, T. Wang, G. Li, Q. Huo and Y. Liu, *Chemical Communications*, 2015.
- [112] S. K. Elsaidi, M. H. Mohamed, H. T. Schaef, A. Kumar, M. Lusi, T. Pham, K. A. Forrest, B. Space, W. Xu and G. J. Halder, *Chemical Communications*, 2015.
- [113] Y.-W. Li, J. Xu, D.-C. Li, J.-M. Dou, H. Yan, T.-L. Hu and X.-H. Bu, *Chemical Communications*, 2015, 51, 14211–14214.
- [114] Y.-S. Bae, J. Liu, C. E. Wilmer, H. Sun, A. N. Dickey, M. B. Kim, A. I. Benin, R. R. Willis, D. Barpaga and M. D. LeVan, *Chemical Communications*, 2014, 50, 3296–3298.
- [115] K. Liu, B. Li, Y. Li, X. Li, F. Yang, G. Zeng, Y. Peng, Z. Zhang, G. Li and Z. Shi, *Chemical Communications*, 2014, 50, 5031–5033.
- [116] R. Li, X. Ren, X. Feng, X. Li, C. Hu and B. Wang, *Chemical Communications*, 2014, 50, 6894–6897.
- [117] F. Wang, H.-R. Fu, Y. Kang and J. Zhang, *Chemical Communications*, 2014, 50, 12065–12068.
- [118] S. Xiong, Y. Gong, H. Wang, H. Wang, Q. Liu, M. Gu, X. Wang, B. Chen and Z. Wang, *Chemical Communications*, 2014, 50, 12101–12104.
- [119] C. Song, Y. He, B. Li, Y. Ling, H. Wang, Y. Feng, R. Krishna and B. Chen, *Chemical Communications*, 2014, 50, 12105–12108.
- [120] J. Qian, F. Jiang, K. Su, J. Pan, Z. Xue, L. Liang, P. P. Bag and M. Hong, *Chemical Communications*, 2014, 50, 15224–15227.
- [121] C. H. Lau, R. Babarao and M. R. Hill, *Chemical Communications*, 2013, 49, 3634–3636.
- [122] J. Luo, J. Wang, G. Li, Q. Huo and Y. Liu, *Chemical Communications*, 2013, 49, 11433–11435.
- [123] J. A. Johnson, Q. Lin, L.-C. Wu, N. Obaidi, Z. L. Olson, T. C. Reeson, Y.-S. Chen and J. Zhang, *Chemical Communications*, 2013, 49, 2828–2830.
- [124] V. Bon, J. Pallmann, E. Eisbein, H. C. Hoffmann, I. Senkovska, I. Schwedler, A. Schneemann, S. Henke, D. Wallacher and R. A. Fischer, *Microporous and Mesoporous Materials*, 2015.
- [125] S. Chaemchuen, K. Zhou, N. A. Kabir, Y. Chen, X. Ke, G. Van Tendeloo and F. Verpoort, *Microporous and Mesoporous Materials*, 2015, 201, 277–285.

- [126] E. Keceli, M. Hemgesberg, R. Gr unker, V. Bon, C. Wilhelm, T. Philippi, R. Schoch, Y. Sun, M. Bauer and S. Ernst, *Microporous and Mesoporous Materials*, 2014, 194, 115–125.
- [127] L. Li, J. Yang, J. Li, Y. Chen and J. Li, *Microporous and Mesoporous Materials*, 2014, 198, 236–246.
- [128] A. Das, M. Choucair, P. D. Southon, J. A. Mason, M. Zhao, C. J. Kepert, A. T. Harris and D. M. D’Alessandro, *Microporous and Mesoporous Materials*, 2013, 174, 74–80.
- [129] R. Sabouni, H. Kazemian and S. Rohani, *Microporous and Mesoporous Materials*, 2013, 175, 85–91.
- [130] X. Wu, Z. Bao, B. Yuan, J. Wang, Y. Sun, H. Luo and S. Deng, *Microporous and Mesoporous Materials*, 2013, 180, 114–122.
- [131] M. Du, C.-P. Li, M. Chen, Z.-W. Ge, X. Wang, L. Wang and C.-S. Liu, *Journal of the American Chemical Society*, 2014, 136, 10906–10909.
- [132] A. M. Fracaroli, H. Furukawa, M. Suzuki, M. Dodd, S. Okajima, F. G andara, J. A. Reimer and O. M. Yaghi, *Journal of the American Chemical Society*, 2014, 136, 8863–8866.
- [133] X. Zhao, X. Bu, Q.-G. Zhai, H. Tran and P. Feng, *Journal of the American Chemical Society*, 2015, 137, 1396–1399.
- [134] W. Cai, T. Lee, M. Lee, W. Cho, D.-Y. Han, N. Choi, A. C. Yip and J. Choi, *Journal of the American Chemical Society*, 2014, 136, 7961–7971.
- [135] J. A. Mason, T. M. McDonald, T.-H. Bae, J. E. Bachman, K. Sumida, J. J. Dutton, S. S. Kaye and J. R. Long, *Journal of the American Chemical Society*, 2015, 137, 4787–4803.
- [136] A. L. Dzubak, L.-C. Lin, J. Kim, J. A. Swisher, R. Poloni, S. N. Maximoff, B. Smit and L. Gagliardi, *Nat Chem*, 2012, 4, 810–816.
- [137] X. Kong, E. Scott, W. Ding, J. A. Mason, J. R. Long and J. A. Reimer, *Journal of the American Chemical Society*, 2012, 134, 14341–14344.
- [138] A. O. Yazaydin, R. Q. Snurr, T.-H. Park, K. Koh, J. Liu, M. D. LeVan, A. I. Benin, P. Jakubczak, M. Lanuza and D. B. Galloway, *Journal of the American Chemical Society*, 2009, 131, 18198–18199.
- [139] P. Canepa, C. A. Arter, E. M. Conwill, D. H. Johnson, B. A. Shoemaker, K. Z. Soliman and T. Thonhauser, *Journal of Materials Chemistry A*, 2013, 1, 13597–13604.
- [140] X.-J. Hou, P. He, H. Li and X. Wang, *The Journal of Physical Chemistry C*, 2013, 117, 2824–2834.
- [141] C. R. Wade and M. Dinc a, *Dalton Transactions*, 2012, 41, 7931–7938.
- [142] P. L. Llewellyn, S. Bourrelly, C. Serre, A. Vimont, M. Daturi, L. Hamon, G. De Weir-eld, J.-S. Chang, D.-Y. Hong and Y. Kyu Hwang, *Langmuir*, 2008, 24, 7245–7250.

- [143] C. P. Cabello, P. Rumori and G. T. Palomino, *Microporous and Mesoporous Materials*, 2014, 190, 234–239.
- [144] L. Li, J. Yang, J. Li, Y. Chen and J. Li, *Microporous and Mesoporous Materials*, 2014, 198, 236–246.
- [145] A. Torrisi, R. G. Bell and C. Mellot-Draznieks, *Microporous and Mesoporous Materials*, 2013, 168, 225–238.
- [146] Q. Lin, T. Wu, S.-T. Zheng, X. Bu and P. Feng, *Journal of the American Chemical Society*, 2011, 134, 784–787.
- [147] E. Keceli, M. Hemgesberg, R. Grünker, V. Bon, C. Wilhelm, T. Philippi, R. Schoch, Y. Sun, M. Bauer, S. Ernst, S. Kaskel and W. R. Thiel, *Microporous and Mesoporous Materials*, 2014, 194, 115–125.
- [148] Y. Yang, R. Lin, L. Ge, L. Hou, P. Bernhardt, T. E. Rufford, S. Wang, V. Rudolph, Y. Wang and Z. Zhu, *Dalton Transactions*, 2015, 44, 8190–8197.
- [149] R. Vaidhyanathan, S. S. Iremonger, K. W. Dawson and G. K. Shimizu, *Chemical communications*, 2009, 5230–5232.
- [150] W.-Y. Gao, W. Yan, R. Cai, L. Meng, A. Salas, X.-S. Wang, L. Wojtas, X. Shi and S. Ma, *Inorganic chemistry*, 2012, 51, 4423–4425.
- [151] L. Ding and A. O. Yazaydin, *Physical Chemistry Chemical Physics*, 2013, 15, 11856–11861.
- [152] C. J. Coghlan, C. J. Sumby and C. J. Doonan, *CrystEngComm*, 2014, 16, 6364–6371.
- [153] Z.-H. Xuan, D.-S. Zhang, Z. Chang, T.-L. Hu and X.-H. Bu, *Inorganic Chemistry*, 2014, 53, 8985–8990.
- [154] R.-R. Cheng, S.-X. Shao, H.-H. Wu, Y.-F. Niu, J. Han and X.-L. Zhao, *Inorganic Chemistry Communications*, 2014, 46, 226–228.
- [155] E. Yang, H.-Y. Li, F. Wang, H. Yang and J. Zhang, *CrystEngComm*, 2013, 15, 658–661.
- [156] T. Li, D.-L. Chen, J. E. Sullivan, M. T. Kozlowski, J. K. Johnson and N. L. Rosi, *Chemical Science*, 2013, 4, 1746–1755.
- [157] G. K. Shimizu, R. Vaidhyanathan and J. M. Taylor, *Chemical Society Reviews*, 2009, 38, 1430–1449.
- [158] R. K. Mah, B. S. Gelfand, J. M. Taylor and G. K. Shimizu, *Inorganic Chemistry Frontiers*, 2015, 2, 273–277.
- [159] J. M. Taylor, R. Vaidhyanathan, S. S. Iremonger and G. K. Shimizu, *Journal of the American Chemical Society*, 2012, 134, 14338–14340.
- [160] N. C. Burtch, H. Jasuja and K. S. Walton, *Chemical Reviews*, 2014, 114, 10575–10612.

- [161] B. S. Gelfand, J.-B. Lin and G. K. Shimizu, *Inorganic Chemistry*, 2015, 54, 1185–1187.
- [162] S. Verma, A. K. Mishra and J. Kumar, *Accounts of Chemical Research*, 2009, 43, 79–91.
- [163] Y. Song, X. Yin, B. Tu, Q. Pang, H. Li, X. Ren, B. Wang and Q. Li, *CrystEngComm*, 2014, 16, 3082–3085.
- [164] J. Thomas-Gipson, G. Beobide, O. Castillo, M. Froba, F. Hoffmann, A. Luque, S. Pérez-Yáñez and P. Román, *Crystal Growth & Design*, 2014, 14, 4019–4029.
- [165] T. Li, D.-L. Chen, J. E. Sullivan, M. T. Kozlowski, J. K. Johnson and N. L. Rosi, *Chemical Science*, 2013, 4, 1746–1755.
- [166] J. An, O. K. Farha, J. T. Hupp, E. Pohl, J. I. Yeh and N. L. Rosi, *Nature Communications*, 2012, 3, 604.
- [167] M. Zhang, W. Lu, J.-R. Li, M. Bosch, Y.-P. Chen, T.-F. Liu, Y. Liu and H.-C. Zhou, *Inorganic Chemistry Frontiers*, 2014, 1, 159–162.
- [168] Y. Zhao, H. Wu, T. J. Emge, Q. Gong, N. Nijem, Y. J. Chabal, L. Kong, D. C. Langreth, H. Liu and H. Zeng, *Chemistry-A European Journal*, 2011, 17, 5101–5109.
- [169] M. A. Gotthardt, S. Grosjean, T. S. Brunner, J. Kotzel, A. M. Ganzler, S. Wolf, S. Brase and W. Kleist, *Dalton Transactions*, 2015, 44, 16802–16809.
- [170] J. Kim, B. Chen, T. M. Reineke, H. Li, M. Eddaoudi, D. B. Moler, M. O’Keeffe and O. M. Yaghi, *Journal of the American Chemical Society*, 2001, 123, 8239–8247.
- [171] L. Du, Z. Lu, K. Zheng, J. Wang, X. Zheng, Y. Pan, X. You and J. Bai, *Journal of the American Chemical Society*, 2012, 135, 562–565.
- [172] D. Wang, B. Liu, S. Yao, T. Wang, G. Li, Q. Huo and Y. Liu, *Chemical Communications*, 2015, 51, 15287–15289.
- [173] T. M. McDonald, W. R. Lee, J. A. Mason, B. M. Wiers, C. S. Hong and J. R. Long, *Journal of the American Chemical Society*, 2012, 134, 7056–7065.
- [174] M. Eddaoudi, D. F. Sava, J. F. Eubank, K. Adil and V. Guillerm, *Chemical Society Reviews*, 2015, 44, 228–249.
- [175] B. A. Al-Maythaly, O. Shekhah, R. Swaidan, Y. Belmabkhout, I. Pinnau and M. Eddaoudi, *Journal of the American Chemical Society*, 2015, 137, 1754–1757.
- [176] F. Wang, H.-R. Fu, Y. Kang and J. Zhang, *Chemical Communications*, 2014, 50, 12065–12068.
- [177] Z. Zhang, Y. Zhao, Q. Gong, Z. Li and J. Li, *Chemical Communications*, 2013, 49, 653–661.
- [178] M. Taddei, F. Costantino, A. Ienco, A. Comotti, P. V. Dau and S. M. Cohen, *Chemical Communications*, 2013, 49, 1315–1317.

- [179] B. Liu, R. Zhao, K. Yue, J. Shi, Y. Yu and Y. Wang, *Dalton Transactions*, 2013, 42, 13990–13996.
- [180] X.-L. Zhao and W.-Y. Sun, *CrystEngComm*, 2014, 16, 3247–3258.
- [181] M. Du, C.-P. Li, C.-S. Liu and S.-M. Fang, *Coordination Chemistry Reviews*, 2013, 257, 1282–1305.
- [182] X. Kong, H. Deng, F. Yan, J. Kim, J. A. Swisher, B. Smit, O. M. Yaghi and J. A. Reimer, *Science*, 2013, 341, 882–885.
- [183] J. Liu, P. K. Thallapally, B. P. McGrail, D. R. Brown and J. Liu, *Chemical Society Reviews*, 2012, 41, 2308–2322.
- [184] Z. Wang, K. K. Tanabe and S. M. Cohen, *Inorganic Chemistry*, 2008, 48, 296–306.
- [185] H. Deng, C. J. Doonan, H. Furukawa, R. B. Ferreira, J. Towne, C. B. Knobler, B. Wang and O. M. Yaghi, *Science*, 2010, 327, 846–850.
- [186] T. Watabe, Y. Nishizaka, S. Kazama and K. Yogo, *Energy Procedia*, 2013, 37, 199–204.
- [187] T. Watabe and K. Yogo, *Separation and Purification Technology*, 2013, 120, 20–23.
- [188] T. Prenzel, M. Wilhelm and K. Rezwani, *Chemical Engineering Journal*, 2014, 235, 198–206.
- [189] M. Auta and B. H. Hameed, *Chemical Engineering Journal*, 2014, 253, 350–355.
- [190] R. K. Motkuri, J. Liu, C. A. Fernandez, S. K. Nune, P. Thallapally and B. P. McGrail, *Industrial Catalysis and Separations*, 2014, 61–103.
- [191] S. M. Cohen, *Chemical Reviews*, 2011, 112, 970–1000.
- [192] W. R. Lee, S. Y. Hwang, D. W. Ryu, K. S. Lim, S. S. Han, D. Moon, J. Choi and C. S. Hong, *Energy & Environmental Science*, 2014, 7, 744–751.
- [193] A. Demessence, D. M. D'Alessandro, M. L. Foo and J. R. Long, *Journal of the American Chemical Society*, 2009, 131, 8784–8786.
- [194] N. Planas, A. L. Dzubak, R. Poloni, L.-C. Lin, A. McManus, T. M. McDonald, J. B. Neaton, J. R. Long, B. Smit and L. Gagliardi, *Journal of the American Chemical Society*, 2013, 135, 7402–7405.
- [195] T. M. McDonald, D. M. D'Alessandro, R. Krishna and J. R. Long, *Chemical Science*, 2011, 2, 2022–2028.
- [196] Y.-S. Bae, J. Liu, C. E. Wilmer, H. Sun, A. N. Dickey, M. B. Kim, A. I. Benin, R. R. Willis, D. Barpaga, M. D. LeVan and R. Q. Snurr, *Chemical Communications*, 2014, 50, 3296–3298.
- [197] Y. Lin, Q. Yan, C. Kong and L. Chen, *Scientific Reports*, 2013, 3.
- [198] L. Ge, L. Wang, V. Rudolph and Z. Zhu, *RSC Advances*, 2013, 3, 25360–25366.

- [199] M. Anbia and V. Hoseini, *Chemical Engineering Journal*, 2012, 191, 326–330.
- [200] M. Anbia and S. Sheykhi, *Journal of Industrial and Engineering Chemistry*, 2013, 19, 1583–1586.
- [201] X. Zhou, W. Huang, J. Miao, Q. Xia, Z. Zhang, H. Wang and Z. Li, *Chemical Engineering Journal*, 2015, 266, 339–344.
- [202] C. Petit and T. J. Bandosz, *Advanced Materials*, 2009, 21, 4753–4757.
- [203] Z. Bian, J. Xu, S. Zhang, X. Zhu, H. Liu and J. Hu, *Langmuir*, 2015, 31, 7410–7417.
- [204] Y. Zhao, M. Seredych, Q. Zhong and T. J. Bandosz, *RSC Advances*, 2013, 3, 9932–9941.
- [205] A. Prabhu, A. Al Shoaibi and C. Srinivasakannan, *Materials Letters*, 2015, 146, 43–46.
- [206] I. Ahmed and S. H. Jhung, *Materials Today*, 2014, 17, 136–146.
- [207] B. Zhen, Q. Jiao, Y. Zhang, Q. Wu and H. Li, *Applied Catalysis A: General*, 2012, 445–446, 239–245.
- [208] W. Lu, K. Henry, C. Turchi and J. Pellegrino, *Journal of The Electrochemical Society*, 2008, 155, A361–A367.
- [209] S. Ntais, A. Moschovi, V. Dracopoulos and V. Nikolakis, *ECS Transactions*, 2010, 33, 41–47.
- [210] H. Li, P. S. Bhadury, B. Song and S. Yang, *RSC Advances*, 2012, 2, 12525–12551.
- [211] B. Xin and J. Hao, *Chemical Society Reviews*, 2014, 43, 7171–7187.
- [212] Y. Chen, Z. Hu, K. M. Gupta and J. Jiang, *The Journal of Physical Chemistry C*, 2011, 115, 21736–21742.
- [213] Q.-X. Luo, M. Ji, M.-H. Lu, C. Hao, J.-S. Qiu and Y.-Q. Li, *Journal of Materials Chemistry A*, 2013, 1, 6530–6534.
- [214] N. A. Khan, Z. Hasan and S. H. Jhung, *Chemistry-A European Journal*, 2014, 20, 376–380.
- [215] K. Fujie, T. Yamada, R. Ikeda and H. Kitagawa, *Angewandte Chemie International Edition*, 2014, 53, 11302–11305.
- [216] K. Fujie, K. Otsubo, R. Ikeda, T. Yamada and H. Kitagawa, *Chemical Science*, 2015.
- [217] A. Aijaz, T. Akita, H. Yang and Q. Xu, *Chemical Communications*, 2014, 50, 6498–6501.
- [218] G. D. Zhang, W. F. Cai, C. J. Xu and M. Zhou, *Chemical Engineering Science*, 2006, 61, 558–568.
- [219] O. Ozkan, A. Calimli, R. Berber and H. Oguz, *Chemical Engineering Science*, 2000, 55, 2737–2740.

- [220] H. Vinke, P. J. Hamersma and J. M. H. Fortuin, *Chemical Engineering Science*, 1993, 48, 2197–2210.
- [221] A. A. C. M. Beenackers and W. P. M. Van Swaaij, *Chemical Engineering Science*, 1993, 48, 3109–3139.
- [222] S. Lu, Y. Ma, C. Zhu and S. Shen, *Chinese Journal of Chemical Engineering*, 2007, 15, 842–846.
- [223] M. Rosu, A. Marlina, A. Kaya and A. Schumpe, *Chemical Engineering Science*, 2007, 62, 7336–7343.
- [224] B. Chen, Y. Ji, M. Xue, F. R. Fronczek, E. J. Hurtado, J. U. Mondal, C. Liang and S. Dai, *Inorganic Chemistry*, 2008, 47, 5543–5545.
- [225] H. Liu, B. Liu, L.-C. Lin, G. Chen, Y. Wu, J. Wang, X. Gao, Y. Lv, Y. Pan and X. Zhang, *Nature Communications*, 2014, 5.
- [226] Z. Lei, C. Dai and W. Song, *Chemical Engineering Science*, 2015, 127, 260–268.
- [227] C. Dai, W. Wei and Z. Lei, *Journal of Chemical & Engineering Data*, 2015, 60, 1311–1317.
- [228] B. Van de Voorde, I. Stassen, B. Bueken, F. Vermoortele, D. De Vos, R. Ameloot, J.-C. Tan and T. D. Bennett, *Journal of Materials Chemistry A*, 2015, 3, 1737–1742.
- [229] H. Wu, T. Yildirim and W. Zhou, *The Journal of Physical Chemistry Letters*, 2013, 4, 925–930.
- [230] M. Bosch, M. Zhang and H.-C. Zhou, *Advances in Chemistry*, 2014, 2014.
- [231] H. Jasuja, N. C. Burtch, Y.-g. Huang, Y. Cai and K. S. Walton, *Langmuir*, 2013, 29, 633–642.
- [232] H. Jasuja and K. S. Walton, *Dalton Transactions*, 2013, 42, 15421–15426.
- [233] H. Jasuja, Y. Jiao, N. C. Burtch, Y.-G. Huang and K. S. Walton, *Langmuir*, 2014, 30, 14300–14307.
- [234] W. Zhang, Y. Hu, J. Ge, H.-L. Jiang and S.-H. Yu, *Journal of the American Chemical Society*, 2014, 136, 16978–16981.